


PREDICTION OF MOMENT CAPACITY OF CONCRETE SLABS SINGLY REINFORCED WITH CARBON FIBER REINFORCED PLASTICS (CFRP) USING SIMULATED ANNEALING

BY

SAMUEL KOLAWOLE BELLO

DEPARTMENT OF CIVIL ENGINEERING,

FACULTY OF ENGINEERING,

AHMADU BELLO UNIVERSITY,

ZARIA , NIGERIA.

DECEMBER, 2014

PREDICTION OF MOMENT CAPACITY OF CONCRETE SLABS SINGLY REINFORCED WITH CARBON FIBER REINFORCED PLASTICS (CFRP) USING SIMULATED ANNEALING

BY

Samuel Kolawole BELLO

MSc/ENG/07182/2010-2011

A THESIS SUBMITTED TO THE SCHOOL OF POSTGRADUATE STUDIES, AHMADU BELLO UNIVERSITY, ZARIA

IN PARTIAL FULFILLMENT OF THE REQUIREMENTS FOR THE AWARD OF A

MASTERS OF SCIENCE (M.SC) DEGREE IN CIVIL ENGINEERING

DEPARTMENT OF CIVIL ENGINEERING,

FACULTY OF ENGINEERING,

AHMADU BELLO UNIVERSITY,

ZARIA, NIGERIA

DECEMBER 2014

DECLARATION

I declare that the work in this thesis entitled Predicting the Resistance Moment of Carbon Fiber Reinforced Plastic for Singly Reinforced Concrete Slabs Using Annealing Models has been carried out by me in the Department of Civil Engineering. The information derived from the literature has been duly acknowledged in the text and a list of references provided. No part of this thesis was previously presented for another degree or diploma at this or any other institution.

Samuel Kolawole BELLO Signature
Date **CERTIFICATION**

This thesis entitled PREDICTING THE RESISTANCE MOMENT OF CARBON FIBER REINFORCED PLASTIC FOR SINGLY REINFORCED CONCRETE SLABS USING ANNEALING MODELS by Samuel Kolawole BELLO meets the regulations governing the award of the degree of Master of Science (Structural Engineering) in the Department of Civil Engineering of the Ahmadu Bello University and is approved for its contribution to knowledge and literary presentation.

Dr. O. S. Abejide
(Chairman, Supervisory Committee) Signature

Date

Dr. I. Abubakar
(Member, Supervisory Committee) Signature Date

Dr. Y. D. Amartey
(Head of Department) Signature Date

Prof. A. Z. Hassan
(Dean, School of Postgraduate Studies) Signature Date

ACKNOWLEDGEMENTS

Firstly, I wish to thank God for His guidance and protection and for making this work a success.

My sincere appreciations go to my lecturers and project supervisors Dr. O. S. Abejide and Dr. I. Abubakar, who supervised this project. I am very much indebted to them not only for their profound pieces of advice, assistance and encouragement, which were very instrumental to the success of this project, but also for their personal concern and provision of materials and ideas throughout the period of its execution.

I wish to also thank all the entire members of Staff of the Civil Engineering Department, Ahmadu Bello University, Zaria for their endeavors towards making the best out of me.

I shall never forget the supports I got from my family, friends and other members of my class and colleagues at work in the progress of this work.

ABSTRACT

Prediction of moment capacity of concrete slabs singly reinforced with carbon fiber reinforced plastics (CFRP) using simulated annealing is looked into. Equations for resistance moment are obtained based on the flexural requirements presented in ACI 440. 1R-06 (2006). These equations are then optimized using the Simulated Annealing (SA) algorithm. The developed algorithm is implemented using Visual Basic for Application (VBA). In addition, identification of design variables, objective function and constraints are also presented. The most important factors which influence the ultimate load carrying capacity of CFRP reinforced concrete structures are- effective depth (d) and breadth (b) of the member, concrete strength (f_c') and the material properties of the CFRP reinforcement. Thus, the ultimate moment of resistance based on concrete failure obtained for a CFRP singly reinforced concrete section is $\boldsymbol{M_u = 0.194bd^2f_c'}$,

this is 22.4% lower than the predicted in the code formulation.

TABLE OF CONTENTS

Page

Title Page ---------- **i**

Declaration ---------- **ii**

Certification ---------- **iii**

Acknowledgement ---------- **iv**

Abstract ---------- **v**

Table of Content ---------- **vi**

List of Tables ---------- **x**

List of Figures ---------- **xi**

Notations ---------- **xii**

1.0 INTRODUCTION ---------- **1**

1.1 Background ---------- **1**

1.2 Statement of the Problem ---- 3

1.3 Justification of Study ---- 4

1.4 Aim and Objectives ---- 4

1.5 Scope and limitations ---- 5

2.0 LITERATURE REVIEW ---- 7

2.1 Introduction ---- 7

2.2 History of FRP Composites ---- 8

2.3 FRP Bars ---- 10

2.3.1 Mechanical and Physical Properties of FRP Bars (Lofgren, 2005) ---- 11

2.4 Use of FRP in Reinforced Concrete ---- 13

2.4.1 Analytical Studies ---- 13

2.4.2 Experimental Studies ---- 19

2.5 Optimization of Reinforced Concrete Structures by Simulated Annealing ---- 20

2.5.1 Work Done on Optimization of CFRP Reinforced Concrete Structures ---- 22

2.5.2 Simulated Annealing Background ---- 23

2.6 Flexural Analysis of CFRP RC Slabs to Obtain Resistance Moment Equations -- 23

2.6.1 Simplified Expressions Recommended by ACI 440.1R-06 ---------- 23

2.6.2 Failure Categories of CFRP Reinforced Concrete Slabs ---------- 26

3.0 METHODOLOGY ---------- 34

3.1 Simulated Annealing Background ---------- 34

3.2 Basic Elements of the Optimization ---------- 35

3.3 Advantages and Reasons for Using SA ---------- 38

3.4 Visual Basic for Application (VAB) ---------- 39

3.4.1 Reasons for Using VBA ---------- 39

3.4.2 Disadvantages of Visual Basic ---------- 40

3.5 Formulation of Objective Function ---------- 40

3.5.1 Transformation of Constrained Optimization to an Unconstrained Optimization -- 40

3.6 Formulation of Constraints ---------- 42

3.6.1 Strength of CFRP Reinforced Concrete in Uni-axial Tension ---------- 42

3.6.2 Constraints on Critical Volume ---- 44

3.6.3 Constraints on Aspect Ratio ---- 45

3.6.4 Constraints on Ultimate Moment ---- 46

3.6.5 Constraints on Tension CFRP ---- 46

3.6.6 Constraints on Shear Strength ---- 47

3.6.7 Constraints on Area and Spacing of Stirrups ---- 48

3.6.8 Constraint for Limiting Span/Depth Ratio for Deflection Control ---- 49

3.6.9 Constraints on Design Variables ---- 50

3.7 Stress in the CFRP ---- 51

3.8 Working Procedure of the Algorithm ---- 52

3.9 Stopping Conditions ---- 53

4.0 RESULTS AND DISCUSION ---- 55

4.1 Input Parameters (Assumed Values) ---- 55

4.2 Simulated Annealing Input Parameters ---- 57

5.0 SUMMARY, CONCLUSIONS AND RECOMMENDATIONS ---------- 64

5.1 Summary ---------- 64

5.2 Conclusions ---------- 64

5.3 Recommendation and Suggestions ---------- 66

REFERENCES ---------- 68

APPENDIX ---------- 76

Compressed Simulated Annealing VBA Code. ---------- 85

LIST OF TABLES

Table 2.1: Advantages and Disadvantages of FRP ---------- 9

Table 2.2: Physical Properties of Fiber ---------- 11

Table 2.3: Coefficients of Thermal Expansion for Reinforcing Bars ---------- 12

Table 2.4: Typical Tensile Properties of Reinforcing FRP Bars ---------- 12

Table 2.5: Chronological Development of Documents for FRP ---------- 19

Table 2.6: Environmental Reduction Factors for Various FRP Bars ---------- 27

Table 2.7: Experimental Moment Capacity by Other Researchers Compare with

Models ---------- 33

Table 4.1: Limiting Values of Assumed Variables ---------- 58

Table 4.2: Optimal Moment Capacity Results Using Simulated Annealing ------- 60

LIST OF FIGURES

Figure 2.1: Usual Tensile Properties of Reinforcing Bars. ---------- 13

Figure 2.2: Rectangular Stress Block---------- ---------- 25

Figure 2.3: Failure Modes of CFRP RC Section---------- 26

Figure 2.4: Strength Reduction Factor and Strain Level (ACI-318-02) ---------- 28

Figure 2.5: Strength Reduction Factor and Reinforcement Ratio (ACI-318-02) ---- 28

Figure 2.6: Balanced Failure Condition (ACI 440.1R-06, 2006) ---------- 30

Figure 2.7: CFRP Rupture Mode (Tension Failure) (ACI 440.1R-06, 2006) --------- 31

Figure 2.8: Concrete Crushing Failure Mode (ACI 440.1R-06, 2006) ---------- 32

Figure 3.1: Flow Chart 1 of a Simple Simulated Annealing Algorithm---------- 36

Figure 3.2: Flow Chart 2 of a Simple Simulated Annealing Algorithm---------- 37

Figure 3.3: Flow Chart for the Algorithm---------- 53

Figure 4.1: Interface for Input Parameters ---------- ---- 56

Figure 4.2: Interface for Simulated Annealing Input Parameters ---------- 58

Figure 4.3: Optimal Moment Capacity Results Using Simulated Annealing- - - - - - - - - 61

Figure 4.4: Performance of the Simulated Annealing Program- 62

NOTATIONS

$\propto (\varepsilon_c)$	Factor to represent the compressive force in concrete
β_1	Factor to define the stress block in compression zone
β_b	Moment distribution ratio, for simply supported slabs $\beta_b = 1$;
ΔE	Difference between the objective function values of the two solutions.
φ	The violation coefficient
ε_2	Strain at which matrix fails
ε_{cu}	Usable compressive strain in concrete
ε_{fu}	Design rupture strain of CFRP reinforcement.
ε_c	Maximum strain in concrete
ρ	Percentage of area of CFRP to area of concrete
ρ_{fb}	Balanced reinforcement ratio
γ_m	Partial factor of safety for material, assumed as 1.5 for concrete in flexure.
ε_{cr}	Strain value corresponding to the matrix cracking stress
τ	Interfacial bond stress between fiber and the matrix
a	Penalty parameter
a_b	Depth of the neutral axis
A_f	Area of CFRP reinforcement
A_{fb}	Area of CFRP required for balanced condition.
A_{fmin}	Minimum area of fiber
A_{svmin}	Minimum stirrup area
A_{svmax}	Maximum stirrup area

A_{freq}	Area of tension CFRP required at mid–span to support ultimate loads,
A_{fprov}	Area of tension CFRP provided at mid-span
a_s	Shear span
$\frac{a_s}{d}$	Effective shear span to depth ratio *b*
	Breadth of the slab
c_b	Neutral axis depth for a balanced cross section
$C_{f,m}$	Volume fraction
c	A temperature factor which is a constant smaller than 1 but close to 1.
C_{cr}.	Critical volume of fiber
C_E	Environmental reduction factor
d	Effective depth of the slab
d_f	Diameter of CFRP
E	System energy
E_{oc}	Initial tangent modulus of concrete in compression,
$E_{f,m}$	Young's modulus of CFRP
E_f	Elastic modulus of CFRP
F	Fiber factor
f_{fu}	Ultimate Stress in CFRP
f_f	Stress in CFRP reinforcement in tension
$f_{c'}$	Cylinder compressive strength of concrete
$f_{t'}$	Splitting cylinder strength of fiber concrete
f_2	Matrix cracking stress
$f_{f'}$	Matrix cracking strain
f_t	Split tensile strength
f_{ck}	Cube strength of concrete
l	Length of fiber
M_n	Nominal moment of the member
m	Number of constraints

S	Spacing of stirrups
T	Temperature
$P(E)$	Probability that the system is in a state of energy E.
$g_i(x)$	Constraint function
V_{un}	Ultimate shear strength of CFRP concrete
V_u	Ultimate shear force applied.
V_{fs}	Shear strength of fiber
V_s	Shear capacity
X_i	Current point during optimization process
X_i^l	Lower limit of input variable
X_i^u	Upper limit of input variable
$Z(x)$	Objective function

CHAPTER ONE

INTRODUCTION

1.1Background

Since the 1970s, researchers have been motivated to investigate alternative solutions to overcome the problem of corrosion phenomenon of concrete structures reinforced with steel (Nawy *et al*., 1977). Though many solutions have come into action, the use of non-metallic materials became one of the promising alternative solutions. Fiber reinforced plastic (FRP) materials are lightweight, thermally non-conductive, exhibit high tensile strength, and have been reported (Nawy *et al*., 1977) to be noncorrosive in nature when compared with conventional steel reinforcement; these composites have been suggested as suitable reinforcement for concrete structures instead of steel. FRP composites are very easy to shape and form, which is always not possible with other high strength materials. FRP composites are anisotropic and possess good strength along the fiber length, but reduced strength across the fiber axis (Benmokrane *et al*., 2010,). The ACI 440 1R-06, (2006) allows the use of CFRP bars as main reinforcement for concrete structures such as bridge decks, floor slabs and wall type structures (abutments, stems and wing walls). In these members, flexural strength is provided by the longitudinal reinforcement and shear strength is provided by the concrete only.

The tensile properties of CFRP reinforcing bars range from 450 to 3500 N/mm^2 and from 38,000 to 300,000 N/mm^2 in terms of Young's modulus and 0.8% to 4.0% in terms of failure strains (Clarke, and O' Regan, 1995). Tensile strength is also influenced by the diameter of the reinforcement, however similar effects do not exist in the case of conventional steel reinforcement (Achillides, 1997).
The use of CFRP reinforcements, in lieu of conventional steel reinforcements requires better understanding under various loading and performance conditions (Benmokrane *et al*., 2010,). Considerable researches have been carried out mainly on CFRP reinforced concrete specimens under monotonically increasing load (Sivagamasundari and Kumaran, 2008). Only limited research works have been carried out on CFRP reinforced concrete specimens under pulsating or repeated loading conditions (Sivagamasundari and Kumaran, 2008).

This work presents the Prediction of moment capacity of concrete slabs singly reinforced with carbon fiber reinforced plastics (CFRP) using simulated annealing by way of simulation using a formulated computer application which finds the optimum value of the objective function -- the optimal moment capacity (k_{opt}), as modeled using the nominal moment equations in the ACI 440 1R-06, (2006) code. The optimum resistance moment of CFRP reinforced concrete sections M_{opt} is then

obtained from k_{opt}.

The parameters that affect the resistance moment of CFRP reinforced concrete slabs include the flexural strength of members, cross sectional properties, geometric and material properties of reinforcing CFRP bars. Among all these properties, the member's effective depth, *d*, breadth, *b*, concrete compressive strength, f_c', and CFRP bar diameter, d_f, are dealt with as the random variables that affect the moment resistance of CFRP reinforced concrete slabs while CFRP reinforcement ratio, is treated as a deterministic design variable in the assessment.

Equations based on the ACI 440 1R-06 (2006) are modeled to predict the nominal strength in flexure of CFRP reinforced concrete slabs. Thus, the simulation involves an optimization problem that maximizes the objective function and predicts the resistance moment of CFRP reinforced slabs. Unlike other optimization problems, here the objective function is considered as the maximization of resistance moment rather than the reduction of cost. The algorithm developed for the optimization is adopted from the method of Simulated Annealing and it is executed using Visual

Basic for Applications, VBA.

1.2Statement of the Problem

Concrete structures face major problems from the deterioration and corrosion of the reinforcing steel. Retrofitting and rehabilitation, instead of replacement, are needed to increase the ultimate strength for those inadequate concrete structures. One of the innovative technologies to strengthen the concrete structures is to use fiber reinforced polymers (FRP). Recently the interest in the application of FRP in reinforced concrete structures has been increasing (Chen and Chung, 1996).

Most of the work done on CFRP are significantly due to its attractive properties, such as high tensile strength, lightweight, corrosion resistance and are concentrated on the retrofitting of reinforced concrete beams and columns (Chen and Chung, 1996). However, very limited tests have been conducted to study the flexural behavior of reinforced concrete slabs strengthened internally by this composite material (Chen and Chung, 1996).

1.3Justification of Study

This work is considered because, asides the well-recognized advantages that CFRP strengthening systems possess, there are also some important doubts about using it; bearing in mind that CFRPs are new materials and not so widely used, there is a need to determine the optimum resistance moment of CFRP in singly reinforced concrete slab sections though a proposal has been given in ISIS (2011).

1.4Aim And Objectives

1.4.1Aim

This work aims at predicting the moment capacity of concrete slabs singly reinforced with carbon fiber reinforced plastics (CFRP) using simulated annealing which can be safely used for their designs.

1.4.2Objectives

The objectives of this work are:

i. To derive an optimum value for the resistance moment of singly reinforced concrete slab sections reinforced with CFRP.

ii. Study the bending behavior of slabs reinforced with CFRP using relevant a simulation technique for the purpose of predicting the optimum resistance moment of CFRP in singly reinforced concrete slab sections which will satisfy the design requirements of ACI 440 1R-06, (2006).

1.5Scope And Limitations

1.5.1Scope

The scope of this work is limited to improving the understanding of the bending behavior of CFRP singly reinforced concrete slabs, obtaining the optimum resistance moment in accordance with ACI 440 1R-06, (2006), design requirements and for their practical applications when CFRP bars are used as reinforcing bars.

1.5.2Limitations

The limitations of this work are:

i. CFRP has not been widely used because of its low ductility as depicted by its elastic modulus.

ii. CFRP bars when loaded in tension, exhibit linear stress-strain behavior up to rupture.

iii. There is no yield point and associated plateau to provide a ductile response when used as tensile reinforcement in concrete, thus they fail abruptly. iv.The absence of plasticity in CFRP materials implies that under-reinforced flexural sections experience a sudden tensile rupture instead of a gradual yielding, as in the case with steel reinforcement. Thus, the concrete crushing failure mode of an over-reinforced member is more desirable, due to enhanced energy absorption and greater deformability leading to a more gradual failure mode. Member recovery is essentially elastic with little or no energy dissipation resulting from large deformations.

v. There have been attempts to improve the ductility of CFRP with little or no success. (Michael, 1997).

vi. The optimum results of a simulated annealing algorithm depends largely on the anneal start temperature and number of iterations.

CHAPTER TWO

LITERATURE REVIEW

2.1 Introduction

So much attention has been focused on the research and development of fiber materials including carbon fibers, aramid fibers, and glass fibers as alternatives to the steel used in reinforced and prestressed concrete. Fiber Reinforced Polymers (FRP) have been increasingly accepted in the construction industry as a promising substitute for steel, this has been obvious especially during the last decade. Civil structures made of steel reinforced concrete are normally susceptible to environmental attacks that lead to electrochemical corrosion of steel

reinforcement, which further leads to deficient structures, and in some cases failures. The advantages of using FRP reinforcement over steel are (Seible and Karbhari, 1996):

(1) Excellent corrosion resistance

(2) High strength-to-weight ratio and

(3) High stiffness-to-weight ratio

Bridges, buildings, off-shore structures, mining operations, chemical plants, highway pavements, geotechnical applications, structural or nonstructural elements are being reinforced, rehabilitated or stabilized with FRP in the form of bars, fabrics and grids (Rostasy, 1996). Constant maintenance and repair is needed to enhance the design life of those structures. Hence, as recently as the 1990s, an outstanding combination of the properties of FRP composites (corrosive resistance, good fatigue and damping resistance and high strength to weight ratio) arose an interest in structural engineers.

Despite their low specific gravity as compared to steel, they possess high tensile strength and many of them provide excellent resistance to the elements of weather and chemical attacks. When used as reinforcing materials, the fibers are usually bonded together with the help of binding agents such as resins and cement, resulting in widely different appearances and compositions (Tang, 1999). Many theoretical and experimental studies (Tang, 1999), have been carried out to check the feasibility of using FRP to reinforce concrete structures. This work is focuses on carbon fibers reinforced plastic (CFRP) materials as reinforcements for singly reinforced concrete slab sections.

2.2 History of FRP Composites

The use of composite materials can be traced back to the use of straw as reinforcement in bricks used by ancient civilizations (e.g. Israelites and Egyptians in 800 BC.) (Tang, 1999). In the United States, short glass fiber reinforcement was used in the early 1930's to reinforce concrete. FRPs are the latest version of this very old idea of making better composite material by combining two different materials (Nanni, 1999). After World War II, US manufacturers began producing fiberglass and polyester resin composites into vehicle hulls and redomes (radar cover). The automotive industry first introduced composites in the early 1950's and since then many components of today's vehicles are been made out of composites. The aerospace industry began to use FRP composites as lightweight material with acceptable strength and stiffness which reduced the weight of aircraft structures such as pressure vessels and containers. Today's modern jets use large components made out of composites as they are less susceptible to fatigue than traditional metals (Nanni, 1999). Other industries like naval, defense and sporting goods have since used advanced composite materials on a widespread basis. In the construction industry, the first application of composites was a dome structure built in Benghazi, Libya in 1968 (Tang, 1999), and other structures followed. Thus, FRP composites have emerged as an alternate

reinforcing material. In Europe, construction of prestressed FRP Bridge in Germany in 1986 was the beginning of the use of FRP (Tang, 1999). More than 100 commercial projects involving FRP reinforcement were undertaken in Japan (ACI 440, 2001). Extended efforts on an international level brought design codes and guidelines for FRP reinforced concrete into existence. FRP design provisions were included in "Recommendation for Design and Construction of Concrete Structures Using Continuous Fiber Reinforced Materials," Japan Society of Civil Engineers, (JSCE), 1997. The Canadian Standards Association (CSA) published a document related to the use of FRP, called CAN/CSA-S806-02. The American Concrete Institute (ACI) presented general design recommendations for flexural concrete elements reinforced with FRP reinforcing bars in ACI 440.1R-06 (2006), "Guide for the Design and Construction of Concrete Reinforced with FRP Bars." ACI also published other documents addressing other composite-related issues (e.g. Strengthening Using Composites (440.2R-02), Testing of Composite Materials (440.3R-04). Table 2.1 gives details of the advantages and disadvantages of using CFRP reinforced concrete sections.

TABLE 2.1: ADVANTAGES AND DISADVANTAGES OF FRP REINFORCEMENT.(Seible and Karbhari, 1996)

Advantages of FRP Reinforcement	**Disadvantages of FRP Reinforcement**
High longitudinal tensile strength (varies with sign and direction of loading relative to fibers)	No yielding before brittle rupture
Corrosion resistance (not dependent on a coating)	Low transverse strength (varies with sign and direction of loading relative to fibers)
Nonmagnetic	Low modulus of elasticity (varies with type of reinforcing fiber
High fatigue endurance (varies with type of reinforcing fiber)	Susceptibility of damage to polymetric resins and fibers under ultraviolet exposure
Lightweight (about 1/5 to ¼ the density of steel	Low durability of glass fibers in a moist environment

	High coefficient of thermal expansion perpendicular to the fibers, relative to concrete
	May be susceptible to fire depending on matrix type and concrete cover thickness

Near Surface Mounted (NSM) FRP rods are also used for repairing and upgrading of reinforced concrete structures. This technique becomes particularly attractive for flexural strengthening in the negative moment regions of slabs and girders where reinforcement could be subjected to the severe damage due to mechanical and environmental conditions (Lorenzis and Nanni, 2002).

2.3 FRP Bars

FRP reinforcing bars are similar to steel rebars in the shape and deformation patterns. They were not commercially available until the late 1970's. Commercially available FRP bars have various types of cross sectional shapes i.e. square, round, solid, dog bone, and hollow. These bars have various deformation systems i.e., exterior wound fiber, sand coatings, and separately formed deformations. FRP bars can be manufactured using various techniques such as pultrusion, braiding, and weaving (ACI Committee 440, 2001).

Table 2.2 Typical Physical Properties of a few Fibers are listed

TABLE 2.1 2. PHYSICAL PROPERTIES OF FIBER FROM LOFGREN (2005)

Table 2.1 2. Physical properties of typical fibre, from Lofgren (2005)

Type of Fibre	Diameter [μm]	Specific gravity [g/cm^3]	Tensile strength [MPa]	Elastic modulus [GPa]	Ultimate elongation [%]
Metallic					
Steel	5-1 000	7.85	200-2 600	195-210	0.5-5
Glass					
E glass	8-15	2.54	2 000-4 000	72	3.0-4.8
AR glass	8-20	2.70	1 500-3 700	80	2.5-3.6
Synthetic					
Acrylic (PAN)	5-17	1.18	200-1 000	14.6-19.6	7.5-50.0
Aramid (e.g. Kevlar)	10-12	1.4-1.5	2 000-3 500	62-130	2.0-4.6
Carbon (low modulus)	7-18	1.6-1.7	800-1 100	38-43	2.1-2-5
Carbon (high modulus)	7-18	1.7-1.9	1 500-4 000	200-800	1.3-1.8
Nylon (polyamide)	20-25	1.16	965	5.17	20.0
Polyester (e.g. PET)	10-8	1.34-1.39	280-1 200	10-18	10-50
Polyethylene (PE)	25-1 000	0.96	80-600	5.0	12-100
Polyethylene (HPPE)	-	0.97	4 100-3 000	80-150	2.9-4.1
Polypropylene (PP)	10-200	0.90-0.91	310-760	3.5-4.9	6-15.0
Polyvinyl acetate (PVA)	3-8	1.2-2.5	800-3 600	20-80	4-12
Natural - organic					
Cellulose (wood)	15-125	1.50	300-2 000	10-50	20
Coconut	100-400	1.12-1.15	120-200	19-25	10-25
Bamboo	50-400	1.50	350-50	33-40	-
Jute	100-200	1.02-1.04	250-350	25-32	1.5-1.9
Natural - inorganic					
Asbestos	0.02-25	2.55	200-1 800	164	2-3
Wollastonite	25-40	2.87-3.09	2 700-4 100	303-530	-

2.3.1 Mechanical and Physical Properties of FRP Bars (Lofgren, 2005)

The mechanical properties of FRP bars are typically quite different from those of steel bars. The properties are dependent on the fiber type, but generally, FRP bars have lower weight, lower Young's Modulus but higher strength than steel. FRP bars have density ranges from 1246 to 2103kg/m³, one sixth to one forth that of steel. The reduced weight eases the handling of FRP bars on the project site (Lofgren, 2005). The longitudinal coefficient of thermal expansion is dominated by fiber properties, while the transverse coefficient is dominated by the resin. Table 2.3 lists the coefficient of thermal expansion for typical FRP bars and steel (Lofgren, 2005).

TABLE 2.3: COEFFICIENTS OF THERMAL EXPANSION FOR REINFORCING BARS (Lofgren, 2005)

COEFFICIENT OF THERMAL EXPANSION, CTE,× $10^{-60}C$				
Direction	Steel	GFRP	CFRP	AFRP

Longitudinal	6.5 (11.7)	3.3 to 5.6 (6.0 to 10.0)	-4.0 to 0.0 (-9.0 to 0.0)	-3.3 to -1.1 (-6 to -2)
Transverse	6.5 (11.7)	11.7 to 12.8 (21.0 to 23.0)	41 to 58 (74.0 to 104.0)	33.3 to 44.4 (60.0 to 80.0)

The tensile properties of FRP are what make them an attractive alternative to steel reinforcement. The tensile strength depends on the fiber-volume fraction, the rate of curing, and the manufacturing process. The tensile properties of a particular FRP bar should be obtained from the bar manufacturer. When loaded in tension, FRP bars do not exhibit any plastic behavior (yielding) before rupture. Table 2.4 (Nanni, 1999) gives the usual tensile properties of reinforcing bars.

TABLE 2.4: TYPICAL TENSILE PROPERTIES OF REINFORCING FRP BARS (Nanni, 1999)

Direction	**Steel**	**GFRP**	**CFRP**	**AFRP**
Nominal Yield Stress, MPa	276 to 517	N/A	N/A	N/A
Tensile Strength, MPa	483 to 690	483 to 1600	600 to 3690	1720 to 2540
Elastic Modulus, GPa	200	35 to 51	120 to 580	41 to 125
Yield Strain, %	0.14 to 0.25	N/A	N/A	N/A
Rupture Strain, %	6.0 to 12.0	1.2 to 3.1	0.5 to 1.7	1.9 to 4.4

Figure 2.1 shows on a graph the usual tensile properties of FRP reinforcing bars.

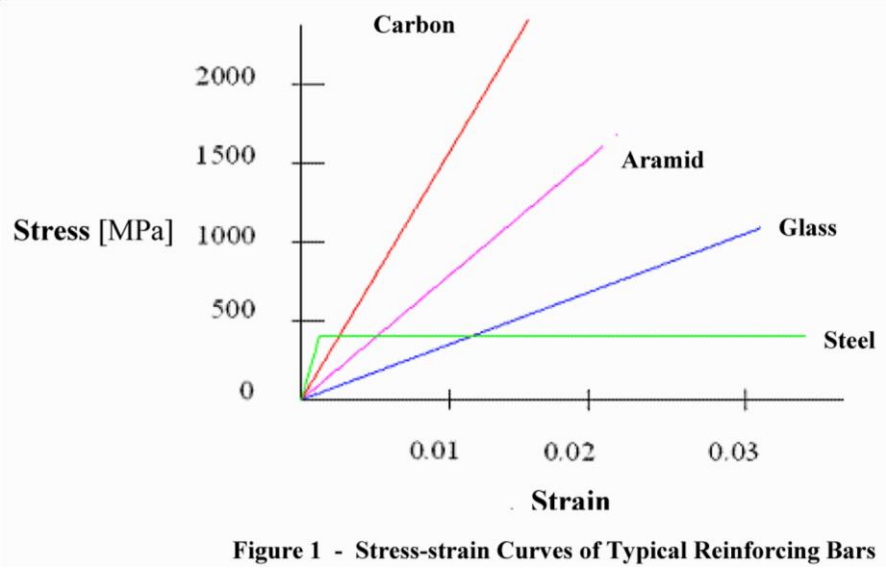


Figure 2.1: *Usual Tensile Properties of Reinforcing Bars (Nanni, 1999).*

The compressive modulus of elasticity of FRP reinforcing bars appears to be smaller than its tensile modulus of elasticity (Nanni, 1999). FRP reinforcing bars subjected to a constant load over time can suddenly fail. This phenomenon is known as creep rupture. In general, carbon fibers are the least susceptible to creep rupture, whereas aramid fibers are moderately susceptible, and the glass fibers are the most susceptible (ACI Committee 440, 2001).

2.4 Use of FRP in Reinforced Concrete

2.4.1 Analytical Studies

The use of FRP bars as tensile reinforcement in concrete structures has been a pressing issue since the early 1990s. Research activities have been carried out to study the behavior of FRP reinforced concrete structures (Nanni, 1999).

2.4.1.1 Use of FRP in Laboratory Reinforced Concrete Construction

Seible and Karbhari (1996) presented the advantages and disadvantages for reinforcing concrete structures using composite materials. The advantages include high static and fatigue strength, resistance to chemicals, and versatility in the fabrication process while the disadvantages include high cost of material, low modulus of elasticity and possible plastic deformation under long term loads of composites in his study. He also gave methods of producing composites and applications of composites. Tegola (1998) compared the behavior of concrete beams or columns reinforced with non-metallic bars to similar members reinforced with steel. In another study by Nanni (1999), composite material properties, FRP forms suitable for concrete reinforcement, applications, installation procedure, and quality control are discussed. The actual FRP system is

installed by sandwiching the dry fiber sheet between two layers of resin. After installing this system, hammer sounding and tap testing are the techniques used to find delaminations between the FRP and the substrate. For some strengthening projects a final quality control step is performed by implementing a load test. Field applications for FRP composite bars as reinforcement for bridge decks are presented by El-Salakawy and Benmokrane, (2004),

2.4.1.2 Bond between FRP Reinforcement and Concrete

A better understanding of the mechanical behavior of FRP reinforcements in particular bond behavior is needed in order to use them for practical purposes. Numerous tests are analyzed to better understand bond mechanisms and the influence of fiber type, outer surface (shape and type of matrix), and other significant parameters on bond performances in Cosenza *et al.,* (1997). Furthermore, the study was aimed at estimating the adequacy of two analytical models for the constitutive bond-slip relationship of FRP rebars in the well-known model by Malvar (1994). In another investigation by Esfahani *et al*., (2005), the results of an experimental study on bond strength of CFRP bars embedded in normal concrete and self-consolidating concrete are presented. Different parameters such as type of concrete, bar situation in specimen, and cover thickness are studied. Based on the experimental results, the author concluded that the splitting bond strength of CFRP reinforcing bar was not less than that of steel bars, and also the bond strength of bottom CFRP reinforcing bars was almost the same for normal concrete and self-consolidating concrete.

2.4.1.3 Flexural Behavior

Flexure has been a widely studied issue. Plevris *et al*., (1995) aimed at developing a fundamental understanding of the time-dependent (creep and shrinkage) behavior of reinforced concrete slab sections strengthened with FRP laminates. An experimental program is also described confirming the analytical analysis. ElMihilmy and Tedesco (2000) investigated the flexural behavior of reinforced concrete beams strengthened with externally bonded FRP laminates. A simple and direct analytical procedure for evaluating the ultimate flexural capacity of FRP strengthened concrete flexural members is given. Another investigation to find the methods for predicting deflections and crack widths in beams reinforced with CFRP bars is presented in Toutanji and Saafi, (2000), Deflections and crack widths obtained from experimental results are compared with those obtained analytically.

An experimental and analytical study on behavior of Carbon Fiber-based rods as flexural reinforcement was conducted by Thiagarajan (2003). The author concluded from the pullout tests that bonding of carbon fiber rods is not a major concern and bond quality increases with bar size. Also, carbon fiber rods have to undergo high strains to develop high stresses; hence, higher strength concrete is better suited for these beams. It was also concluded that the experimental crack widths are smaller than the crack widths predicted using the ACI 440 (2001) crack width equation. The study by Yost *et al.,* (1993)

evaluates the flexural performance of simply supported beams reinforced with a 2D fiber-reinforced plastic grid considering the main parameter as the amount of longitudinal FRP. Experimental results are compared with theoretical predictions calculated according to traditional steel-reinforced concrete procedures which conclude that flexural capacity can be accurately predicted. In another investigation (Li *et al*., 2002) introduced new Engineered Cementitious Composite (ECC) to replace brittle concrete matrix.

Experimental results have shown that ECC beams exhibit significant increases in flexural performance in terms of ductility, load-carrying capacity, shear resistance, and damage tolerance compared with the counterpart high-strength concrete beam. Several researchers also studied the use of FRP to reinforce masonry structures. Unreinforced masonry (URM) buildings are vulnerable to earthquakes. Bajpai and Duthinh (2003) focused their research on strengthening and retrofitting of existing masonry walls with near mounted, non-corrosive fiber reinforced polymer bars. The research established the effectiveness of near surface mounted rods in strengthening concrete masonry walls and provides design guidelines for out-of-plane flexure and in-plane shear.

2.4.1.4 Shear Behavior

Chajes *et al*., (1995) focused on the effects of externally applied composite fabrics on the shear capacity of concrete beams. In their study, parameters such as, strength and stiffness of a variety of woven composite fabrics along with their orientation are studied. The use of near surface mounted (NSM), FRP rods is a promising technology for increasing flexural as well as shear strength of deficient reinforced concrete structures. In a study by Lorenzis and Nanni (2002), tensile and bond tests are carried out on carbon FRP deformed rods for application as NSM reinforcement to strengthen beams in shear and the results are compared with the prediction of a simple design approach. In a recent study by Whitehead and Ibell (2001), an analytical approach to investigate the shear response of FRP reinforced and prestressed concrete has been developed based on equilibrium and compatibility across a shear discontinuity. Correlation between the analytical and experimental results is better than predictions of current guideline provisions for prestressed concrete beams containing FRP reinforcement.

2.4.1.5 Design Approaches

Design guidelines for FRP reinforced concrete structures have been developed in Japan (JSCE, 1997), Canada (ISIS, 2001; CSA-S806, 2002), USA (ACI 440.1R01, 2001; ACI440.1R-03, 2003; ACI 440.1R-06, 2006), and Europe (Sivagamasundari and Kumaran, 2008),Table 2.5 gives a summary of the historical development of the existing documents ruling the design of internal FRP reinforced concrete structures.

Triantafillou and Antonopoulos (2000) described a simple design model for calculating the contribution of FRP sheets to the shear capacity of strengthened reinforced concrete elements. It is demonstrated that the contribution of FRP sheets to shear capacity is typically controlled by the maximum effective strain. Newhook *et al*., (2002), conducted a parametric study on rectangular and Tsections to show that the design based on allowable strain in the FRP results in sections that exhibit large deformation before failure. Amy (2002) presented design methods for FRP strengthened concrete using sheets or NSM bars. Grace and Singh (2003) presented another design approach for bridge beams prestressed with carbon FRP bars. They examined the effect of the reinforcement ratio and the level of prestressing forces on the deflections and ultimate load carrying capacity of a double-T beam specimen. ACI Committee 440 (2001) provides recommendations for the design and construction of FRP reinforced concrete structures. ACI 440.1R-06 (2006) gives a general information on the history and use of FRP reinforcement, material properties of FRP, and committee recommendations on the engineering of concrete reinforced with FRP bars.

TABLE 2.5: CHRONOLOGICAL DEVELOPMENT OF DOCUMENTS FOR FRP (Sivagamasundari *et al*, 2008)

Table 4 - Chronological Development of Documents for Internal FRP Reinforcement

1970s	**1996**	**1997**
Use of fiber reinforcement in concrete	The European Committee for Concrete (EUROCRETE) published a set of design recommendations for FRP RC	The Japan Society of Civil Engineers (JSCE) published a set of design recommendations for FRP RC
1999	**2000**	**2001**
The Swedish National code for FRP RC was published	The Canadian Standard Association (CSA) published a set of design recommendations for FRP RC Bridges (CAN/CSA S6-00)	The ISIS Canada published a manual on the use of internal FRP reinforcement The American Concrete Institute (ACI) Committee 440 published the first version of design recommendations for internal FRP reinforcement (440.1R)
2002	**2003**	**2006**
The CSA published a set of design recommendations for FRP RC Buildings (CAN/CSA S806-02) CUR Building & Infrastructure published a set of design recommendations for FRP RC (The Netherlands)	ACI Committee 440 published the second version of guidelines 440.1R	The National Research Council (CNR) published the Italian design recommendations for internal FRP reinforcement (CNR-DT 203/2006) ACI Committee 440 published the third version of guidelines 440.1R

2.4.2 Experimental Studies

The research by Pecce *et al.*, (2000), proved experimentally that the Bernoulli's hypothesis (plane sections remain plane) is valid for concrete sections reinforced with FRP bars. The research was based on the experimental testing of three simply supported concrete beams. The cross-sectional dimensions were 500 mm wide, 185 mm high. The beams were tested using four-point loading for a span length of 3400 mm. The beams were reinforced by CFRP bars and were designed to have a dominant flexural behavior reducing the shear influence. Beams with less amount of FRP reinforcement showed lower stiffness. It is proved that the reinforcement amount can be important, not only for increasing the flexural capacity, but also for serviceability purposes.

Ferreira *et al*., (2001) reported a numerical model for the analysis of concrete shell structures reinforced with FRP rebars. Experiments on concrete beams reinforced with FRP rebars are performed to analyze the accuracy of the predictions obtained by the numerical model. Three point bending tests of concrete beams using different reinforcement ratios were executed. The results obtained show the importance of their bar geometry on the structural behavior. Dog-bone sections yielded higher failure loads and delayed cracking when compared with circular sections.
Kocaoz *et al*., (2005), studied the optimal design of singly reinforced concrete structures reinforced with carbon FRP bars. This work reports the optimization of the resistance moment of CFRP for singly reinforced slabs. An optimization algorithm is developed using the Simulated Annealing (SA) Optimization process and the developed algorithm is executed using Visual Basic for Applications (VBA).

2.5 Optimization of Reinforced Concrete Structures by Simulated Annealing

A review of structural optimization can be found in the study by Cohn and Dinovitzer (1994), who pointed out that there was a gap between theoretical studies and the practical application in practice. They also noted the short number of studies that concentrated on concrete structures. A review of structural concrete optimization can be found in the study by Sarma and Adeli (1998). The methods of structural optimization may be classified into two broad groups: exact methods and heuristic methods. The exact methods are the traditional approach, they are based on the calculation of optimal solutions following iterative techniques of linear programming (Rajeev and Krisnamoorthy, 1992). The second main group comprises the heuristic methods, whose recent development is linked to the evolution of artificial intelligence procedures. This group includes a broad number of search algorithms (Yepes and Medina, 2006), such as genetic algorithms, simulated annealing, threshold accepting, tabular search, ant colonies, etc. These methods have been successful in areas different to structural engineering (Yepes and Medina, 2006). They consist of simple algorithms, but require a great computational effort, since they include a large number of iterations in which the objective function is evaluated and the structural restrictions are checked.

Among the first studies of heuristic optimization applied to structures, the contributions of Jenkins (1992) and of Rajeev and Krisnamoorthy, (1992) are to be mentioned. Both authors applied genetic algorithms to the optimization of the weight of steel structures. As regards reinforced concrete structures, applications include the work of Coello *et al*., (1997), who applied genetic algorithms to the economic optimization of reinforced concrete beams. Recently, there has been a number of reinforced concrete applications (Yepes *et al*., 2006) which optimize reinforced concrete beams and building frames by genetic algorithms. However, despite

advances on structural concrete optimization, present design-office practice of concrete structures is much conditioned by the experience of structural engineers.
Most procedures are based on the adoption of cross-section dimensions and material grades based on sanctioned common practice. Once the structure is defined, it follows the analysis of stress resultants and the computation of passive and active reinforcement that satisfy the limit states prescribed by concrete codes. Should the dimensions or material grades be insufficient, the structure is redefined on a trial and error basis. Such process leads to safe designs, but the economy of the concrete structures is, therefore, very much linked to the experience of the structural designer.

2.5.1 Work Done on Optimization of CFRP Reinforced Concrete Structures

In spite of performing various optimization techniques for reinforced concrete structures by various researchers data on the algorithms developed using simulated annealing for structural optimization of fiber reinforced concrete structural elements are much limited. Optimization techniques for the element level of reinforced concrete structures have been presented for example in Adamu and Karihaloo, (1994). These methods were based on sequential linear programming, continuum- type optimality criteria, and nonlinear programming such as Powell's algorithm. Recently the discrete optimization of structures has been performed using Genetic Algorithms (Adamu, and Karihaloo, 1994). Very little literature is available in the field of fiber reinforced concrete structural optimization because design methods for FRP are yet to be fully developed, though some guidelines are available for its applications to airfield pavements and some hydraulic structures (Hwan, 1992). So is the case with standard test procedures to be adopted for testing and evaluation of the performance of FRP elements. Ezeldin *et al*., (1992), optimized reinforced fibrous concrete beams using direct search technique. The algorithm conducts a systematic search in the space of four variables which include beam width, beam depth, fiber content, and aspect ratio of fibers to yield an optimum solution for a given objective function. It is therefore the main objective of this research to develop an algorithm using simulated annealing that performs a search for the optimum resistance moment of CFRP reinforced concrete.
Unlike other optimal design problems, here the primary objective function is considered as the maximization of resistance moment rather than the cost. The flow chart for the general simple simulated annealing is given in Figures 2.15 and 2.16

2.6 FLEXURAL ANALYSIS OF CFRP REINFORCED CONCRETE SLABS TO OBTAIN RESISTANCE MOMENT EQUATIONS

2.6.1 Simplified Expressions Recommended by ACI 440.1R-06 (ACI Committee, 2006)

The flexural capacity of concrete members reinforced with CFRP bars can be calculated based on assumptions similar to those made for members reinforced with steel bars. Both concrete crushing and CFRP rupture are acceptable failure modes in governing the design of CFRP reinforced concrete slabs provided that strength and serviceability criteria are satisfied. The flexural capacity of a singly reinforced section will be governed by:

(i) Rupture of the CFRP tension reinforcement in which case, the section is referred to as an under-reinforced section.

(ii) Crushing of the concrete where the section is referred to as an over-reinforced section and

(iii) Simultaneous failure of both the concrete and the tension reinforcement, in which case the section is referred to as a balanced section. This case is also referred to as a balanced strain condition.

2.6.1.1 Assumptions in the ACI Method

The assumptions for design of a singly reinforced concrete section in the ACI code are given as follows (ACI 440.1R-06, 2006)

1. A plane section before loading remains plane after loading.
2. The maximum usable compressive strain in the concrete is assumed to be 0.003mm/mm.
3. The tensile strength of the concrete is ignored.
4. The tensile behavior of the FRP reinforcement is linearly elastic until failure.
5. Perfect bond exists between concrete and FRP reinforcement.
6. A rectangular stress block is used for concrete in compression as shown in

Figure 2.2.

7. The compressive force equals the tensile force.

8. The internal moment equals the applied bending moment.

The analysis presented is based on the conventional compatibility and equilibrium conditions used for normal reinforced concrete except that the material properties of
CFRP are put into consideration.

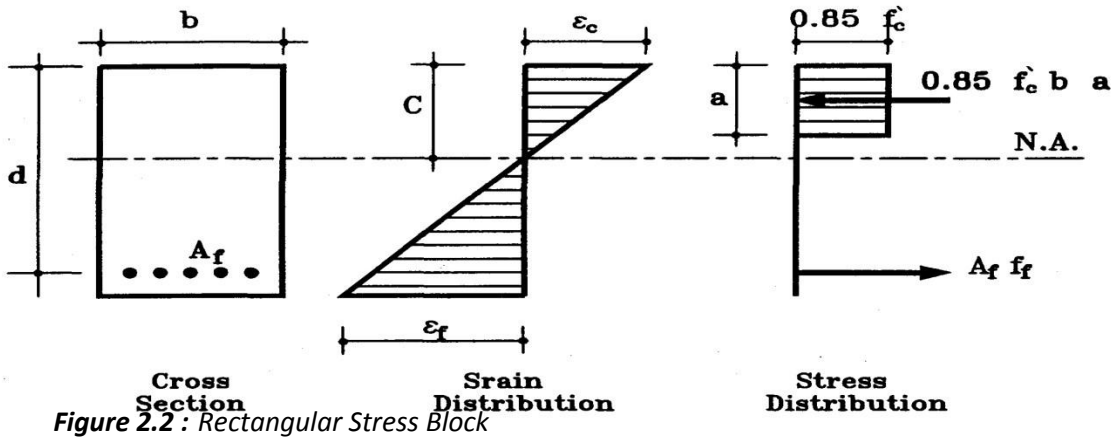


Figure 2.2 : *Rectangular Stress Block*

Sections with smaller amounts of reinforcement fail by CFRP tensile rupture, while larger amounts of reinforcement result in failure by crushing of the compression-zone concrete prior to the attainment of ultimate tensile strain in the outermost layer of CFRP reinforcement (Triantafillou and Antonopoulos, 2000). The absence of plasticity in CFRP materials implies that under-reinforced flexural sections experience a sudden tensile rupture instead of a gradual yielding, as in the case with steel reinforcement. Thus, the concrete crushing failure mode of an over-reinforced member is somewhat more desirable, due to enhanced energy absorption and greater deformability leading to a more gradual failure mode. Member recovery is essentially elastic with little or no energy dissipation resulting from large deformations.

The Whitney rectangular stress block is adequate for flexural capacity prediction when crushing of compression-zone concrete occurs in over-reinforced sections, provided that strain compatibility is used to determine CFRP tensile forces. If CFRP tensile rupture controls failure, the Whitney stress block may not be applicable, unless compression-zone concrete is at near-ultimate conditions. An equivalent stress block that approximates the actual stress distribution in the concrete at CFRP rupture can be used, or the moment capacity can be determined using an estimated tension force moment arm. Compression-zone FRP reinforcement is not considered

effective for increasing moment capacity, enhancing ductility, or reducing long-term deflections (El-Mihilmy *et al*., 2000).
In Figure 2.3, the two types of failure may be accounted for; 'area 1' is when the ultimate CFRP strain is reached and 'area 2' is when the concrete ultimate compressive strain is reached (Clarke, 1996).

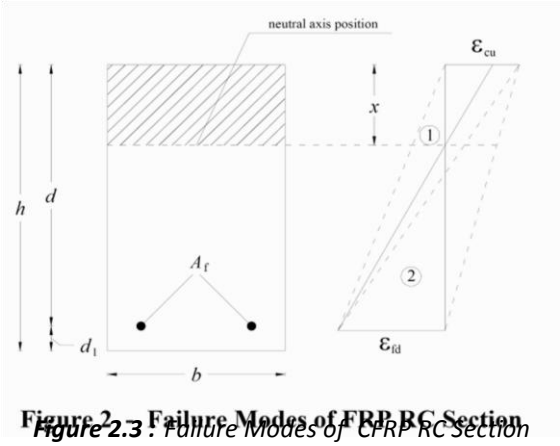


Figure 2.3 : Failure Modes of FRP RC Section
***Figure 2.3** : Failure Modes of CFRP RC Section*

Since CFRP reinforcement exhibits linear stress-strain behavior, the ultimate failure mode of CFRP reinforced concrete slab has to be based upon the nature of failure, magnitude of energy absorption, and other advantages or disadvantages.

2.6.2 Failure Categories of CFRP Reinforced Concrete Slabs

Long term exposure to various types of environments can reduce the tensile strength, creep rupture, and fatigue endurance of CFRP bars, hence, material properties used in design equations should be reduced based on the type and level of environmental exposure. Table 2.6 gives the environmental reduction factors (ACI 440 R-96, 1996).

TABLE 2.6: ENVIRONMENTAL REDUCTION FACTORS FOR VARIOUS FRP BARS

Exposure Condition	Fiber Type	Environmental Reduction Factor CE
Concrete not Exposed to Earth and Weather	Carbon	1
	Glass	0.8
	Aramid	0.9
Concrete Exposed to Earth and Weather	Carbon	0.9
	Glass	0.7
	Aramid	0.8

The design tensile strength should be determined by,

$$f_{fu} = C_E f^*_{fu} \quad (2.1)$$

Where f^*_{fu} is guaranteed tensile strength of CFRP bar, and f_{fu} is the design tensile strength of CFRP (ACI 440 R-96, 1996).

2.6.2.1 ACI-318 (2002) Design Requirement

The Equation 2.2 given below indicates the safety criterion for design of reinforced concrete sections as also shown, Figures 2.4 and 2.5 are shown below

$$M_u \leq \emptyset M_n \quad (2.2)$$

Where:

M_u= factored ultimate moment based on appled loads times load factors

M_n= nominal flexural strength

$\emptyset$ = strength reduction factor

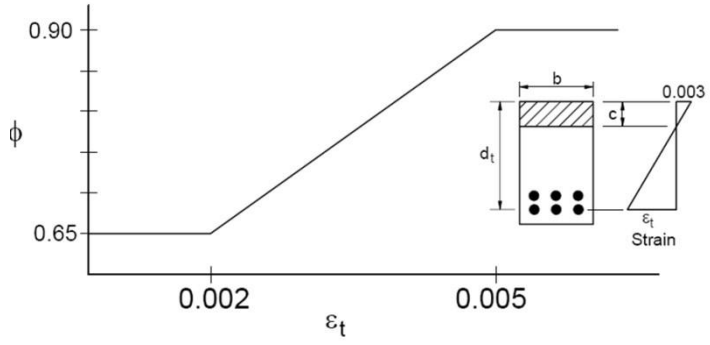


Figure 2.4:*Strength Reduction Factor and strain level (ACI-318-02)*

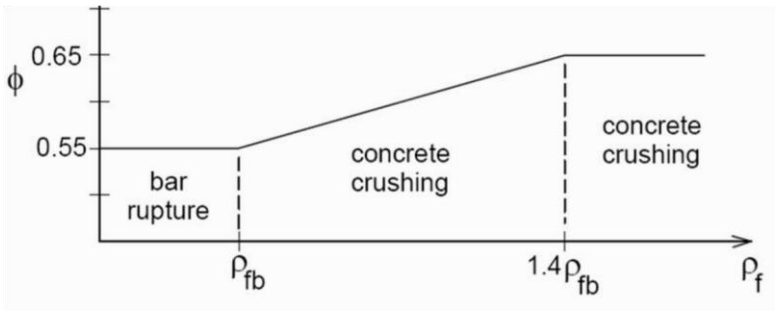


Figure 2.5:*Strength Reduction Factor and reinforcement ratio (ACI-318-02)*

Failure mode can be determined by comparing the CFRP reinforcement ratio, ρ_f and Equation (2.3) to the balanced reinforcement ratio, ρ_{fb}, which is the ratio where concrete crushing and CFRP rupture occur simultaneously as described in Figure 2.6 and Equation (2.4).

2.6.2.2 Balanced Failure

Balanced failure condition is defined as the situation, where strains in concrete and CFRP bars simultaneously reach their predefined limiting values, i.e., $_c = 0.003$ and $_f = \frac{f_f}{E_f}$, in concrete and CFRP bars, respectively. Although the balanced failure condition is difficult to achieve in practice, the concept of balanced failure helps in defining the tension and compression failure modes. The CFRP reinforcement ratio, ρ_f to the amount of concrete in a section is given as

$$\rho_f = \frac{A_f}{bd} \tag{2.3}$$

where, $A_f$is CFRP reinforecment area,*b* and *d* are breadth and depth of slab respectively.

Also, the balanced reinforcement ratio can be expressed as (ACI 440.1R-06, 2006)

$$\rho_{fb} = 0.85\beta_1 \frac{f_c'}{f_{fu}} \left(\frac{E_f \varepsilon_{cu}}{E_f \varepsilon_{cu} + f_{fu}} \right) \tag{2.4}$$

where, f_c' is specified compressive strength of concrete, $_{cu}$ is ultimate strain in concrete, E_f is guaranteed modulus of elasticity of CFRP, and β_1 is an equivalent rectangular stress block parameter taken as 0.85 for $f_c' = 28N/mm^2$, but

$$\beta_1 = 0.85 - 0.05\left(\frac{f_c' - 27.6}{6.7}\right) \geq 0.65 \leq 0.85 \quad (2.5)$$

$f_c' = (20\ to\ 60kN/mm^2)$, for this work

if

$\rho_f \leq \rho_{fb}$, CFRP Rupture failure mode governs (2.6)

$\rho_f > \rho_{fb}$, CFRP Rupture failure mode governs (2.7)

Figure 2.6 shows the balanced failure condition mode for a CFRP reinforced concrete.

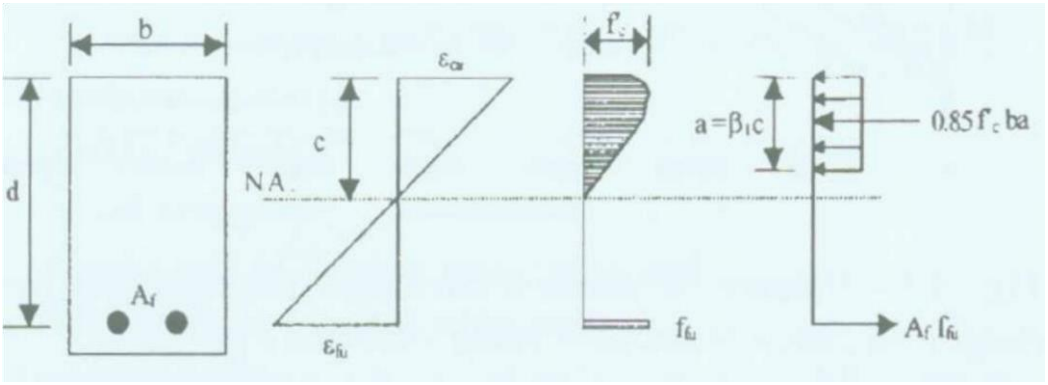


Figure 2.6: *Balanced Failure Condition (ACI Committee, 2006)*

2.6.2.3 Tension Controlled Failure

Tension failure in CFRP reinforced concrete slab sections results in bar rupture leading to catastrophic failure. In case of steel reinforced concrete slabs, primary tension failure may consist of steel yielding which might manifest into either secondary compression failure or tension steel rupture in highly under-reinforced sections. In CFRP reinforced concrete sections, either primary tension failure in the form of bar rupture or primary compression failures are observed. Other failure modes such as concrete cover failure, debonding, etc., are not discussed herein. Since the failure of the member is initiated by rupture of FRP bar, the ACI stress block is not applicable, because the maximum concrete strain (0.003) is not attained (Figure 2.7) (ACI Committee, 2006). The analysis involving unknowns, concrete

compressive strain at failure, depth to the neutral axis, and rectangular stress block parameters becomes complex. A simplified and conservative calculation of the nominal flexural capacity of the members can be based on the following Equations 2.8 and 2.9 obtained through force equilibrium and linear strain variation considerations as shown in Figure 2.7 (ACI Committee, 2006):

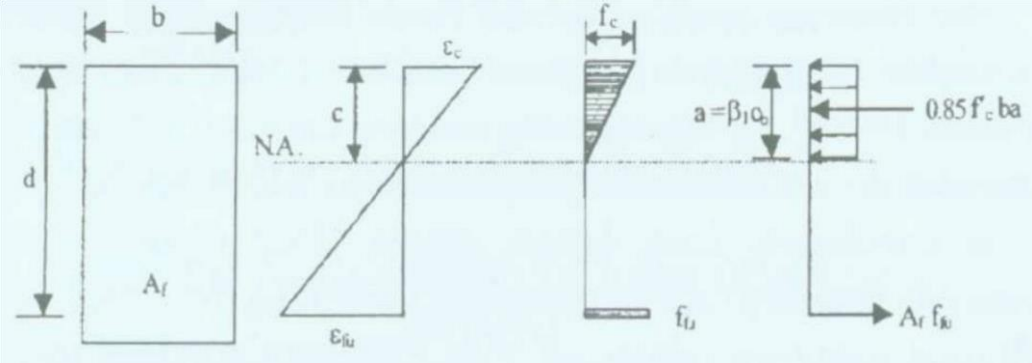


Figure 2.7: *CFRP Rupture Mode (Tension Failure)(ACI Committee, 2006)*

$$M_n = A_f f_{fu}\left(d - \frac{\beta_1 c_b}{2}\right) \tag{2.8}$$

and

$$c_b = \left(\frac{\varepsilon_{cu}}{\varepsilon_{cu}+\varepsilon_{fu}}\right) d \tag{2.9}$$

where,

c_b = neutral axis depth for a balanced cross section

fu = design rupture strain of CFRP reinforcement.

A_f= Area of CFRP reinforcement

f_{fu}=Ultimate Stress in CFRP *d* = effective depth of the slab *a* = depth of the neutral axis

2.6.2.4 Compression Controlled Failure

In the case of compression failures, minimum reinforcement is dictated by a reinforcement ratio to avoid tension failure. Thus the moment capacity of a concrete section having compression failure can be calculated using Equations (2.10) and (2.11) obtained through force equilibrium and expressing CFRP strains in terms of the known concrete strain at failure. This is represented in Figure 2.8 (ACI 440.1R06, 2006)

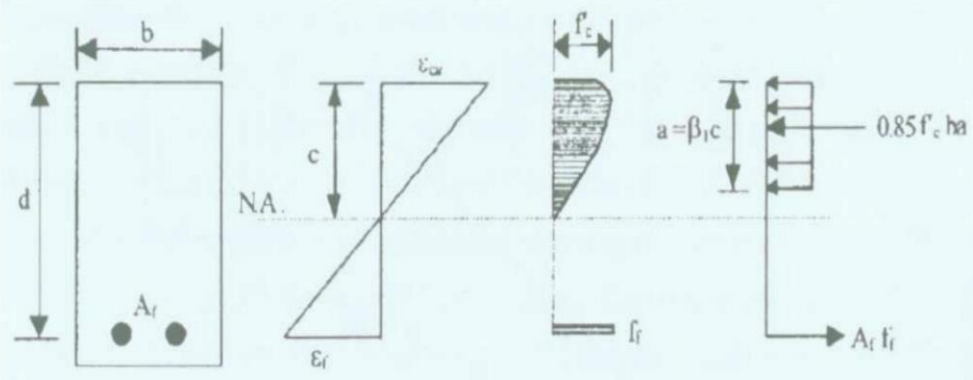


Figure 2.8 : *Concrete crushing failure Mode (ACI 440.1R -06)* (ACI Committee, 2006)

$$f_f = \sqrt{\left(\frac{(E_f \varepsilon_{cu})^2}{4} + \frac{0.85\beta_1 f_c'}{\rho f} E_{f\ cu}\right)} - 0.5E_{f\ cu} \tag{2.10}$$

$$M_n = \rho_f f_f \left(1 - 0.59\frac{\rho_f f_f}{f_c'}\right) bd^2 \tag{2.11}$$

where

M_n= Nominal moment of the member
f_f= stress in CFRP reinforcement in tension

Values of experimental nominal moment of CFRP reinforced concrete slabs in tension and compression failures have been compared with analytical results obtained from Equations (2.8) to (2.9), for various cross-sections, bar dimensions and properties, reinforcement ratios and concrete grades as shown in Table 2.7. These equations will be appropriately used in implementing the simulated annealing optimization algorithm.

TABLE 2.7: EXPERIMENTAL MOMENT CAPACITY BY OTHER RESEARCHERS COMPARED WITH RESULTS FROM MODELS

S/N		1						2				3	
Investigator		Swamy And Al-Ta' An [17]						Buing O' [4]				Veerendra Kumar et al [20]	
Slab No		DR 11	DR 12	DR 21	DR 22	DR 31	DR 32	S1V1	S1V2	S2V1	S2V 2	Series 2 Set 2	Series 3 Set 2
Size		b=1000mm, D=100mm, d= 80mm $E = 151684.66N/mm^2, f_c' = 20$						b=1000mm, D=150mm, d = 120mm $E = 151684.66N/mm^2, f_c' = 30$				b=1000mm, D= 200mm, d = 180mm $E = 151684.66N/mm^2, f_c' = 30$	
Tension Flexural	Area, $A_f, (m^2)$	78.55	78.55	176.74	176.74	78.55	78.55	113.11	227.00	227.00	95.04	63.63	78.5
	Tensile Strength f_f, N/mm^2	2000	2000	2000	2000	2200	2200	2400	2400	2400	2400	2010	2015
$M_{u\ Author}$ (kNm)		12.534	12.534	19.913	19.913	13.787	13.787	32.495	46.319	46.319	27.305	22.962	34.387
FAILURE TYPE		CFRP Rupture	CFRP Rupture	Conc. Crushing	Conc. Crushing	CFRP Rupture	CFRP Rupture	CFRP Rupture	Conc. Crushing	Conc. Crushing	CFRP Rupture	CFRP Rupture	CFRP Rupture
$M_{u\ Exp.}$ (kNm)		16.043	14.288	21.506	21.705	15.855	15.304	34.770	61.604	54.193	31.674	25.029	38.857
FAILURE TYPE		CFRP Rupture	CFRP Rupture	Conc. Crushing	Conc. Crushing	CFRP Rupture	CFRP Rupture	CFRP Rupture	Conc. Crushing	Conc. Crushing	CFRP Rupture	CFRP Rupture	CFRP Rupture
$\frac{M_{u\ Exp.}}{M_{u\ Author}}$		1.28	1.14	1.08	1.09	1.15	1.11	1.07	1.33	1.17	1.16	1.09	1.13

CHAPTER THREE

METHODOLOGY

3.1 Simulated Annealing Background

The simulated annealing algorithm was derived from statistical mechanics. Kirkpatric *et al*., (1980) proposed an algorithm that is based on the analogy between the annealing of solids and the problem of solving combinatorial optimization problems. Annealing is the physical process of heating up a solid and then cooling it down slowly until it crystallizes. The atoms in the material have high energies at high temperature and have more freedom to arrange themselves. As the temperature is reduced the atomic energy decreases. A crystal with regular structure is obtained at the state where the system has minimum energy. If the cooling is carried out very quickly, which is known as rapid quenching, wide spread irregularities and defects are seen in the crystal structure. The system does not reach the minimum energy state and ends in poly crystalline state, which has higher energy. At a given temperature, the probability distribution of system energy is determined by the Boltzmann probability below (Kirkpatric *et al*., 1980):

$$P(E) \propto e^{[-El(kT)]} \tag{3.1}$$

where *E* is system energy, *k* is Boltzmann's constant , *T* is temperature and *P(E)* is the probability that the system is in a state of energy *E*. At high temperatures *E* converges to 1 for all energy states according to Equation (3.1). It can also be seen that there exists a small probability that the system might have high energy even at low temperatures. Therefore, the statistical distribution of energies allows the system to escape from local minimum.

3.2 Basic Elements of the Simulated Annealing Optimization

In the analogy between a combinatorial optimization problem and the annealing process, the states of solid represent feasible solutions of the optimization problem, the energies of the states correspond to the values of the objective function computed at those solutions, the minimum energy state corresponds to the optimal solution to the problem and rapid quenching can be viewed as local optimization.

The algorithm consists of a sequence of iterations. Each iteration consists of randomly changing the current solution to create a new solution in the neighborhood of the current solution. The neighborhood is defined by the choice of the generation mechanism. Once a new solution is

created, the corresponding change in the objective function is computed to decide whether the newly produced solution can be accepted as the current solution. If the change in the objective function is negative the newly produced solution is taken as negative. Otherwise, it is accepted according to Metropoli's criterion based on Boltzmann's probability as stated in Equation (3.1). According to Metropoli's criterion if the difference between the objective function values of the current and the newly produced solutions is equal to or larger than zero, a random number*(δ)* in [0,1] is generated from a uniform distribution and if

$$(\delta) \leq e^{-\frac{\Delta E}{T}} \tag{3.2}$$

then the newly produced solution is accepted as the current solution. If not the current solution is unchanged as expressed in Equation (3.2), Δ*E* is the difference between the objective function values of the two solutions.

The flow chart for the simulated annealing algorithm is presented in Figures 3.1 and 3.2.

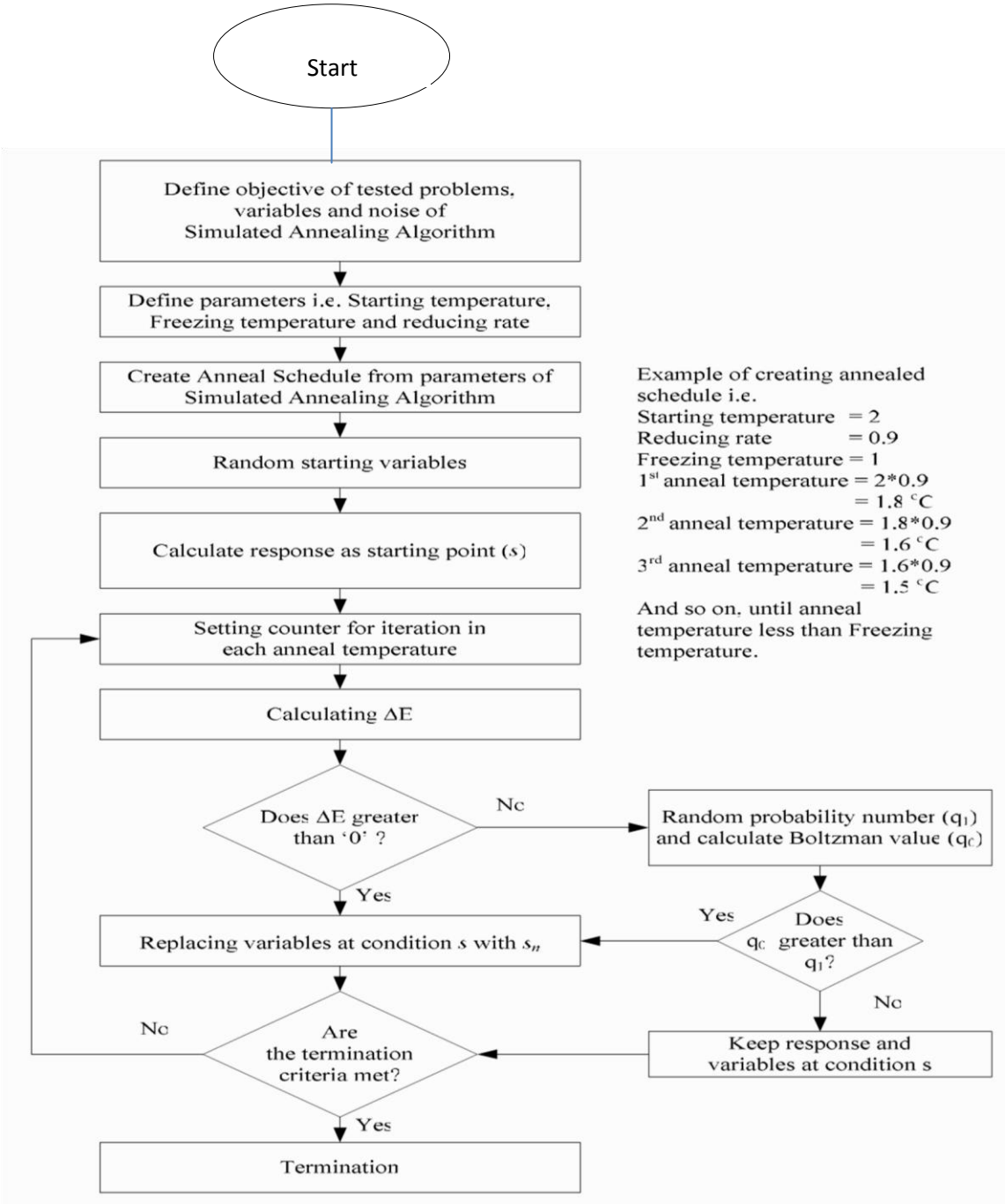


Figure 3.1: *Flow chart 1 of a simple simulated annealing* *algorithm (Kirkpatric et al., 1980)*

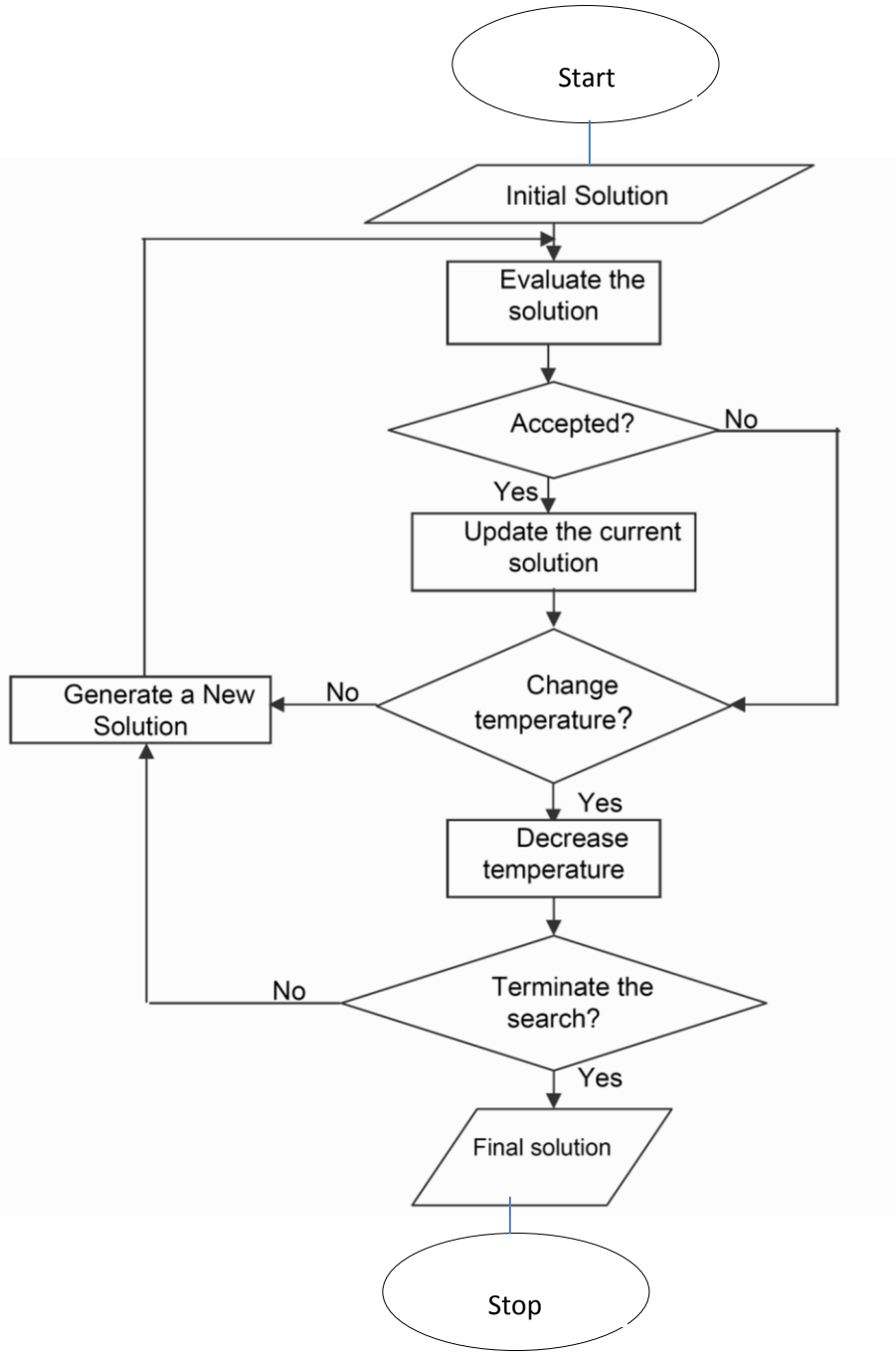


Figure 3.2: *Flow chart 2 of a simple simulated annealing algorithm(Kirkpatric et al., 1980)*

In order to implement the algorithm for a problem there are four principle choices that must be made. These are:

i. Representation of solutions.

ii. Representation of objective function.

iii. Defining the generation mechanism for the neighbors. iv. Designing a cooling schedule.

Solution representation and cost function definitions are as for genetic algorithms. Various generation mechanisms could be developed that again could be borrowed from genetic algorithms, for example mutation and inversion.

In designing the cooling schedule for a simulated annealing algorithm, four parameters must be specified. These are an initial temperature, a temperature update rule, the number of iterations to be performed at each temperature step and a stopping criterion for the search.
There are several cooling schedules adopted in this work. These employ different temperature updating schemes, of these, stepwise, continuous and non-monotonic temperature reduction schemes include very simple cooling strategies. One example is the geometric cooling rule. This rule updates the temperature by the following formula

$$T_{i+1} = cT_i i = 0,1 \ldots .. \quad (3.3)$$

where c is a temperature factor which is a constant smaller than 1 but close to 1.

3.3 Advantages and Reasons for Using Simulated Annealing

Although great success has been achieved during the past decades in structural optimization, these techniques generally have difficulties in avoiding local minima and results are sometimes dependent upon the choice of the initial values in the design space (Kirkpatric *et al*., 1980*)*. With recent advances of computer technology, combinatorial optimization techniques have emerged. Genetic Algorithm (GA) and Simulated Annealing (SA) are quite popular among them and they can efficiently solve the optimization problems with higher probability.
The SA can be characterized by finding a global minimum of an objective function by combining gradient decent with a random process. It is also capable of escaping local minima in addition to more probability to converging local minimum. Design variables constituting set of configured iterations can be of any type that real or discrete, and consequently the searching nature of SA does not require continuity or derivative functions (Kirkpatric *et al*., 1980).

3.4 Visual Basic for Application (VBA)

VBA, which stands for *Visual Basic for Applications,* is a programming language developed by Microsoft. Excel (1993), along with the other members of Microsoft Office, includes the VBA language In a nutshell, VBA is the tool used to develop programs that control many other programs like Excel. VB is a programming language that allows the creation of standalone executable programs (.EXE files).

3.4.1 Reasons for Using VBA

The reasons for using the VBA are follows:

1. Due to the flexibility of VBA, it is a very powerful optimization tool
2. Visual Basic is an easy to learn Programming language than other languages like C++ and yet it is a powerful programming language. Things that may be difficult to program with other language can be done in Visual Basic very

   easily.
3. With Visual Basic, windows based applications and games can be designed.
4. Because Visual Basic is so popular, there are many good resources (books, web sites, news groups and more) that can help in learning and using the language.

5. Many tools on VBA can be found (Sharewares and Freewares) on the internet that will save some programming time, for example, if you want to ping (a ping is like a buzz to get the attention of a user over the internet in your program), instead of writing the ping function yourself, you can download a control that does it, and use it in your program.

6. Compared to other languages, Visual Basic has the widest variety of tools that can be downloaded from the internet and used in programming.

3.4.2 Disadvantage of Visual Basic:

The disadvantage of visual basic is that it is much slower than other programming languages.

3.5 Formulation of Objective Function

3.5.1Transformation of a Constrained to an Unconstrained Optimization

Simulated annealing is ideally suited for unconstrained minimization optimization problems. As the present problem is a constrained maximization problem, we need to make two transformations. The first is to transform the original constrained problem into an unconstrained problem, using the concept of penalty function. A formulation based on the application of penalty whenever there is a violation of specified constraints, is used for

transformation. Here, if the design variable set violates the constraint then a lower value of say 1.0 will be assigned and if not, a higher value say
10.0 is assigned as violation parameter. The violation coefficient "φ" is computed as follows:

$$\varphi = \sum_{i=1}^{m} \varphi_i \tag{3.4}$$

$$\varphi_i = a.\, g_i(x) \tag{3.5}$$

where

$g_i(x) < 0, a = 10; and g_i(x) \geq 0, a = 1.0$

$m = number of constraints$

$a = penalty parameter$

$g_i(x) = constraint function$

The objective function then becomes

$$Z_m(x) = Z(x) + \varphi \tag{3.6}$$

where $Z(x)$ is the objective function subject to :

$$X_i^l \leq X_i \leq X_i^u \quad i = 1, 2 \ldots., n \tag{3.7}$$

$X_i^l = lower\ limit$

$X_i^u = upper\ limit$

The objective function (k_{opt}) for this study is the maximization of moment capacity *(k)* of CFRP reinforced concrete slabs, equations for the nominal moment have been derived in Equations (2.1) to (2.11);

$$\Rightarrow k_{opt} = maximise\ \left[\frac{M_u}{bd^2 f_{cu}}\right] \tag{3.8}$$

Then the optimized ultimate moment is given by

$$M_u = k_{opt} bd^2 \tag{3.9}$$

The second transformation is to transform the maximization problem into a minimization problem. The maximization of a function *Z(x)* is equivalent to the minimization of the negative of the same function. For example, the objective function: Minimize *Z(x)* is equivalent to

$$\text{Maximize } Z'_m(x) = -Z'_m(x) \tag{3.10}$$

3.6 Formulation of Constraints

3.6.1 Strength of CFRP Reinforced Concrete in Uni-axial Tension

According to Cooper *et al*., (1971), the fracture of a composite under tension can be classified into two categories namely single fractures and multiple fractures. A composite fails by a single fracture if both the components are fractured at the same point along their axis, and in this case the composite will immediately break into two pieces. Multiple fracture occurs only if only one of the components is fractured while the other intact. In this case, as the applied stress is increased, more and more cracks will appear in the damaged component until finally the other components is also fracture. In this case, it is physically obvious that during the interval between the appearance of the first crack in the weaker component and the final fracture, the applied stress will produce a larger strain than that produced in the perfect composite. In other words, during this interval the composite will behave in a partially plastic fashion. Thus, the behavior of the composite will be similar to that of a ductile metal and the stress at which the first crack appears in the weaker component can be considered to be the yield stress of the composite.
Following Cooper *et al*., (1971), we can derive a simple criteria for the occurrence of single and multiple fractures in two-component composites.
Considering a two – component cylindrical composite under a tension along its axis. We shall assume that both the components are parallel to each other and to the axis of the cylindrical composite. The two components will be identified by the subscripts
'*m*' and '*f*'. In the case of fiber composite, for example, one of the components will be the fibers and the other will be the matrix.
Let $C_{f,m}$and $E_{f,m}$ denote the volume fraction ($C_f = \frac{V_f}{V}$; $C_m = \frac{V_m}{V}$) and the Young's modulus respectively, of the fibers and matrix. Suppose that a longitudinal stress '*f*' produces uniform strain 'ε' in the composite. So long as ε is small, so that both the components and, hence the composite are in stage I or the elastic zone that is, up to a certain value of the stress, the strain will be proportional to the stress provided cross sectional area remains constant. We can write the following equation with the help of the law of mixtures:

$$f = C_f E_f + C_m E_m \tag{3.11}$$

Let ε_2 denote the strain at which matrix fails. Assuming elastic behavior throughout the region $0 \leq \varepsilon \leq \varepsilon_2$, the value of f at $\varepsilon = \varepsilon_2$ is given by

$$f'_c = C_f E_f \varepsilon_2 + C_m E_m \varepsilon_2 \tag{3.12}$$

$$f_c' = C_f E_f \varepsilon_2 + C_m f_2 \quad (3.13)$$

$$f_c' = C_f f_f' + C_m f_2 \quad (3.14)$$

where $f_2 = E_m \varepsilon_2$ and we have also assumed that 'ε_1', the failure strain of fiber component, is larger than 'ε_2'. The stress in fibers at the strain level corresponding to the matrix cracking strain is given as, f_f', where $f_f' = E_f \varepsilon_2$.

f_c' = f as given by Equation (3.14), is the stress in the composite at which the matrix will fail.

Thus, the conditions for single and multiple fractures can be written as

Single fracture:

$$C_f f_{fu} < f_c' \quad (3.15)$$

Multiple fractures:

$$C_f f_{fu} > f_c' \quad (3.16)$$

where $f_{fu} = E_f \varepsilon_1 \varepsilon$ is the stress in the fiber at its failure strain 'ε_1' or in other words it is the ultimate fracture strength of fibers.

In the case of a multiple fracture, i.e. when as in Equation (3.15), $C_f f_{fu} > f_c'$ is satisfied, the critical stress at which the whole composite will fail is given by

$$f_{cu} = C_f f_{fu}. \quad (3.17)$$

In this case as discussed earlier, the composite will behave like a ductile metal even if both the components (fiber and matrix) are brittle.

3.6.2 Constraints on Critical Volume

The tensile response of fiber–cement composites significantly depends on the volume fraction of the fibers used. The response of fiber reinforced composite up to the cracking strength of the matrix can be described using Equation (3.13). Beyond this point assuming that the matrix does not contribute any further, the strength of the composite is a function of the strength and volume fraction of the fiber as given in Equation (3.16). At a fiber loading up to the critical volume, the release of a matrix cracking load onto the fibers causes the exhaustion of fiber strength; failure is thus by the formation of a single crack. For high volume fractions, the fibers are able to carry load in excess of matrix cracking load; thus the ultimate strength of the composite is higher than the matrix strength, and distributed cracking can exist. The transition from single cracking to multiple cracking takes place above a certain fiber volume fraction, referred to as the critical volume fraction 'C_{cr}'. It has been derived here in by equating Equation (3.13) and (3.16) as given below:

$$C_f f_f' + C_m f_2 = C_f f_{fu} \quad (3.18)$$

Since

$$C_f + C_m = 1 \quad (3.19)$$

$$C_f f_f' + (1 - C_f) f_2 = C_f f_{fu} \quad (3.20)$$

Where f_f', f_2 and f_{fu} are already defined in the previous section. Solving for 'C_f' and taking $C_f = C_{cr}$ the following equation is obtained.

$$C_{cr} = \frac{f_2}{f_{fu}+(f_2-f_f')} \tag{3.21}$$

From the above equation we can conclude that to ensure multiple cracking in the composite, the volume fraction of fibers incorporated in the matrix must be greater than or equal to the critical volume, C_{cr}.

3.6.3 Constraints on Aspect Ratio

To utilize the fracture strength of fibers there should be excellent bond between fiber and the matrix. If a fiber of diameter *'d'* and length *'l'* is to fracture at its mid-length, the bond strength developed over the length $l/2$ must be greater than the fracture strength, i.e.,

$$\frac{\tau\pi dl}{2} \geq \frac{\pi d^2}{4} f_{fu}$$

$$\frac{l}{d} \geq \frac{f_{fu}}{2\tau} \tag{3.22}$$

Thus,

$$A_{sp} \geq \frac{f_{fu}}{2\tau}$$

3.6.4 Constraints on Ultimate Moment

To ensure safety, Equation (2.2) must be satisfied. That is, $M_u \leq \emptyset M_n$

3.6.5 Constraints on Tension CFRP

Providing excessive reinforcement in slabs can result in congestion, thereby adversely affecting the proper placement and compaction of concrete. Excess CFRP reinforcement also results in over reinforced sections .To provide ductile failure, the member should be designed for A_f less than $0.75A_{fb}$, where A_{fb}= area of CFRP required for balanced condition.

It may be found by applying the equilibrium and strain compatibility conditions Equation (3.23), that is,

$$A_{fmax} = 0.75A_{fb} \tag{3.23}$$

where

$$A_{fb} = bd\left[0.85\beta_1 \frac{f_c'}{f_{fu}}\left(\frac{E_f\varepsilon_{cu}}{E_f\varepsilon_{cu}+f_{fu}}\right)\right] \tag{3.24}$$

in which,

f_c' = Cylinder compressive strength of concrete

$_{cu}$= Usable compressive strain in concrete *b* = breadth of the slab *d* = effective depth of the slab; other variables as defined earlier.

That a minimum area of tension reinforcing CFRP is required in flexural members not only to resist possible load effects, but also to control cracking in concrete due to shrinkage and temperature variations. This can be obtained by equating the cracking moment of the section (using the modulus of rupture of CFRP concrete) to the strength computed as a reinforced CFRP concrete section. As recommended by Narayanan and Darwish, (1987), this value is taken as

$$A_{f\,min} = bd\left[\frac{400}{f_f}\right] \tag{3.25}$$

3.6.6 Constraints on Shear Strength

Several studies have shown that the CFRP are particularly effective in providing reinforcement against shear stresses in conventionally reinforced concrete. It is evident from the test results of various authors that stirrups and fibers can be used effectively in combination.

The equation proposed by Narayanan and Darwish, (1987), has been used here to predict the ultimate shear strength of CFRP reinforced concrete slabs, as given in Equation (3.26)

$$V_{fs} = e\left(0.24f_t' + 80\rho\frac{d}{a}\right) + 4.56F \;\; N/mm^2 \tag{3.26}$$

where

$\frac{a}{d}$= effective shear span to depth ratio

$f_{t'}$= Splitting cylinder strength of fiber concrete ρ = Percentage of area of CFRP to area of concrete

F = fiber factor $= \left(\left(\frac{l}{d}\right)C_f\right)f$, where *f* = 0.5 for round fibers, 0.75 for crimped fibers, and 1.0 for fibers with deformed ends (Narayanan and Darwish, 1987).

The method proposed in ACI (1989) code is used for calculating the contribution of stirrups (V_s) to the shear capacity, to which is added the resisting force of concrete from the CFRP; that is, V_{fs} obtained from Equation (3.25)

$$V_s = A_{fv}f_f\left(\frac{d}{S}\right) \tag{3.27}$$

d = Effective depth of the slab *S* = Spacing of stirrups

f_f = Yield stress of CFRP stirrups

The constraint to check the safety of the concrete against shear is given as

$$V_u \leq V_{un} \tag{3.28}$$

Where $V_{un}$is ultimate shear strength of CFRP concrete and V_u is ultimate shear force applied.

3.6.7 Constraints on Area and Spacing of Stirrups

The minimum and maximum stirrup area is taken as proposed in ACI (1989) Code

$$A_{sv\ min} = \frac{50bS}{f_f} \tag{3.29}$$

and

$$Asvmax = 5(Asvmin) \tag{3.30}$$

The constraint on stirrup spacing is formulated based on the assumption that the stirrup spacing '*S* ' varies from $\frac{d}{2}$ down to $\frac{d}{4}$.

The code's objective in recommending such minimum shear reinforcement is to prevent sudden formation of an inclined crack in an unreinforced (or very lightly reinforced) web, possibly leading to an abrupt failure. Further, the provision of nominal web reinforcement restrains the growth of inclined shear cracks, improves the dowel action of the longitudinal tension bars, introduces ductility in shear and provides a warning of the impending failure (Narayanan and Darwish, 1987).

3.6.8 Constraint for Limiting Span/Depth Ratio for Deflection Control

Excessive deflections in slabs are generally undesirable as they cause psychological discomfort to the occupants of the building, and also lead to excessive crack-widths and subsequent loss of durability. The selection of cross sectional sizes of flexural members is often provided by the need to control deflections under service loads.

To formulate the constraint for limiting span/depth ratio for deflection control, limits for serviceability limit state of deflection set out in BS 8110: Part 2 (1985) clause 3.2.1 is used. It is stated in the code that the deflection is noticeable if it exceeds span/250. The code states that the basic span to effective depth ratios for rectangular and flanged slabs is so determined as to limit the total deflection to span/250. For simply supported slabs, spans up to 10*m*, the basic value is taken as 20. If the span exceeds 10*m* the basic value is multiplied by 10/span in meters. Depending on the area and the stress of steel for tension reinforcement, the basic value shall be modified by multiplying with the modification factor given by the formula in the code:

$$\text{Modification Factor} = 0.55 + \frac{477 - f_s}{120\left(0.9 + \left(\frac{M_u}{bd^2}\right)\right)} \leq 2.0 \tag{3.31}$$

Note that the amount of tension reinforcement present is measured by the term $\frac{M_u}{bd^2}$ and f_s is taken as f_f

The service stress is estimated from the Equation (3.32), that is:

$$f_f = \frac{5 f_f A_{f\,req}}{8 A_{f\,prov}} \left(\frac{1}{\beta_b}\right) \tag{3.32}$$

Where A_{freq} is the area of tension CFRP required at mid–span to support ultimate loads, A_{fprov} is the area of tension CFRP provided at mid-span and

$$\beta_b = \frac{\text{moment after redistribution}}{\text{moment before redistribution}} \tag{3.33}$$

For simply supported slabs $\beta_b = 1$;
To satisfy the deflection limits

$$\frac{Actual\ Span}{d} \leq \frac{Allowable\ span}{d} \tag{3.34}$$

3.6.9 Constraints on Design Variables

The design constraints are formulated herein as follows

$$b_{min} \leq b \leq b_{max} \tag{3.35}$$

$$d_{min} \leq d \leq d_{max} \tag{3.36}$$

$$f_{fmin} \leq f_f \leq f_{fmax} \tag{3.37}$$

$$f'_{c\,min} \leq f'_c \leq f'_{c\,max} \tag{3.38}$$

where
$b_{min},\ b_{max},\ d_{min}, d_{max},\ f_{f\,min},\ f_{f\,max}, f'_{c\,min},\ f'_{c\,max}$ represent the lower and upper bound values of variables , breadth (b), slab depth, (*d*), CFRP diameter, (d_f) and Compressive Strength of Concrete, (f'_c).

3.7 Stress in the CFRP

The method of calculation of stress in fiber corresponding to the failure strain of matrix is given below. In the pre-cracking stage, the influence of matrix cracking in the composite is neglected. It is assumed that the carbon fiber bonds perfectly with the concrete matrix and no slippage occurs at the fiber–matrix interface. Since carbon fibers have minor effect on compressive strength, the compressive model for plain concrete as recommended in BS 8110-1985:Pt.1 and EC2 (2008) is adopted for CFRP concrete. The initial tangent modulus of concrete in compression, E_{oc} as given in the above recommendation is as follows:

$$E_{oc} = 5.5 \left[\frac{f_{cu}}{\gamma_m}\right]^{0.5} \tag{3.39}$$

where γ_m is the partial factor of safety for material. Here, this value is assumed as 1.5 for concrete in flexure.

The strain value corresponding to the matrix cracking stress (f_2) can be calculated as follows:

$$_{cr} = \frac{f_2}{E_{oc}} \tag{3.40}$$

Assuming perfect bond between the matrix and fiber and uniform strain throughout the composite, the stress in fiber at the strain level corresponding to the matrix cracking strain is given as

$$f_f' = E_{f\ cr} \tag{3.41}$$

3.8 Working Procedure of the Algorithm

The simulated annealing algorithm starts with a "high" temperature, T_0. A sequence of design vectors is then generated randomly until equilibrium is reached; that is, the average value of 'Z_m.' reaches a stable value as '*i*' increases. The best point reached is recorded as X_{oppt}. Once thermal equilibrium is reached, the temperature *T* is reduced and a new sequence of moves is made and continued until a sufficiently low temperature is reached, at which stage no more improvement in the objective function value can be expected. The basic algorithm is shown as a flow diagram in Figure 3.3. Starting from an initial vector X_1, the algorithm generates successively improved points randomly X_2, X_3,.... moving toward the global maximum solution. If X_i, denotes the current point, random moves are made along each coordinate direction, in turn. The new coordinate values are uniformly distributed around the corresponding coordinate of X_i,. One half of these intervals along the coordinates are stored as the step vector, S_i. If the point falls outside the range given in Equation (3.7) a new point satisfying the equation is found. A candidate design vector *X* is accepted or rejected according to criteria known as the Metropolis criterion (Equation 3.2).

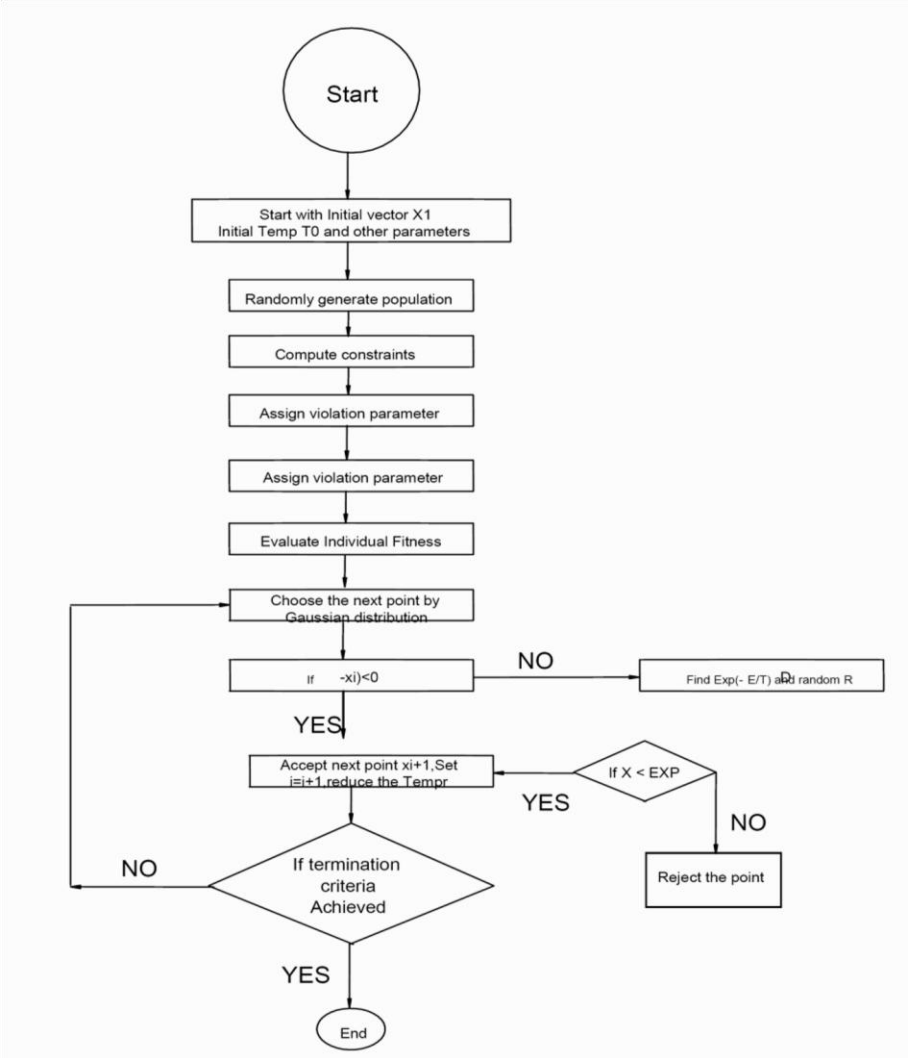


Figure 3.3: *Flow chart for the algorithm*

3.9 Stopping Conditions

If the simulated annealing is terminated too early, a suboptimal solution will be obtained, while if the simulated annealing is terminated too late, the extra iterations take up computational time. There are a number of stopping conditions which include
(Ingber, 1995):

(1) When a maximum number of iterations has been exceeded.

(2) When no improvement occurs over a number of iterations.

(3) When a certain percentage of the simulated annealing is around an optimum.
(4) When the objective function slope is approximately zero.

The SA has been employed to the optimization of the resistance moment of singly reinforced sections and the procedures followed are listed in the following sections.

CHAPTER FOUR

RESULTS AND DISCUSSION

The concrete structure analyzed in this work is a CFRP singly reinforced concrete slab section with an assumed geometry. The model for the resistance moment of the slab is obtained from ACI-440-1R (2006) code and simulated using the Simulated
Annealing (SA) algorithm. The developed algorithm was then implemented using Visual Basic for Applications (VBA).

4.1 Input Parameters (Assumed Values)

The following are the assumed values of various parameters used in the program. The values are obtained from suggested data in the ACI-440-1R (2006) and known properties of CFRP and concrete from experience. These are:

Tensile strength of CFRP = $2068.42 N/mm^2$
Tensile Strain of CFRP $= 0.5$

Interfacial bond stress between fiber and the matrix (τ) =7.0 N/mm^2
Shear span $a_s = 0.84\ m$
Split tensile strength$(f_t) = 0.1 f_c'$
Stress value corresponding to failurestrain of matrix $(f_2) = 1.412\ f_f$

Elastic modulus of CFRP $E_f = 1.5 \times 10^5 N/mm^2$

The first interface when using the developed application is shown in Figure 4.1, this interface is used for inputting parameters which define the CFRP properties, slab properties and the simulation upper and lower bounds. These parameters define the objective function of the simulation to the program so that searching space and time are limited within these bounds. Each of the input boxes is linked to the VBA code and sends the values inputted by the user to the codes. The command button “Run
Simulation” activates the codes to start the simulation, while the command button “Exit”, terminates the code at any point while it is running.

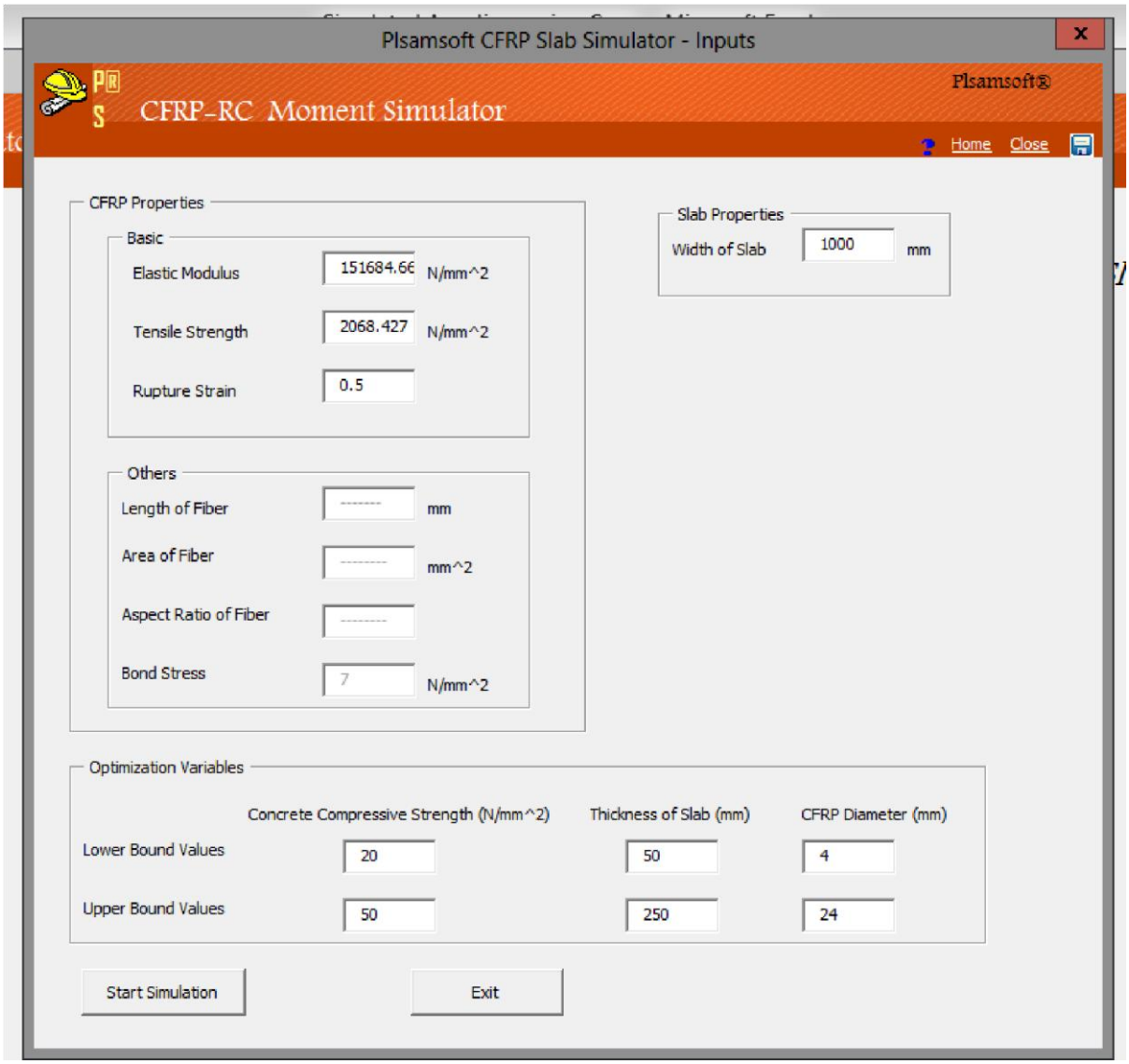


Figure 4.1: *Interface for Input parameters*

4.2 Simulated Annealing Input Parameters

The various simulated annealing parameters used are as follows:
Starting value of Temperature (T_0) = 500
No of iterations (niter) = 100
Temperature reducing rate (c) = 0.99
No of variables (nvar) = 4
The starting temperature is taken as 500 because during the annealing process, the time spent at each temperature level must be sufficiently long to allow the system to reach a thermal equilibrium or a steady state. If care is not taken in adhering to the annealing temperature schedule, undesirable random fluctuations may cause the shift of the ground state. The basic idea of statistical mechanics initiates a generalization of the iterative improvements or the

search for a better solution of the combinatorial optimization. This process is encountered to a 'Steepest-Descent' algorithm for
Minimization problems or a 'Steepest-Ascent' algorithm for maximization problems, in this case the temperature reducing rate (c) is taken as 0.99.
Number of iterations is taken as 1000 because it is expected that convergence will be achieved before the 1000th iteration when the objective function converges to a steady and maximum value. It can also be set at 100,000 but the minimum which is 1000 is used.

Number of variables (nvar) is taken as 4, since the program searches in a space of 4 variables, width of slab *(b),* effective depth of slab *(d),* diameter of CFRP, (d_f) and compressive strength of concrete$f_c'(kN/mm^2)$, this also limits the searching time of the program during the simulation.

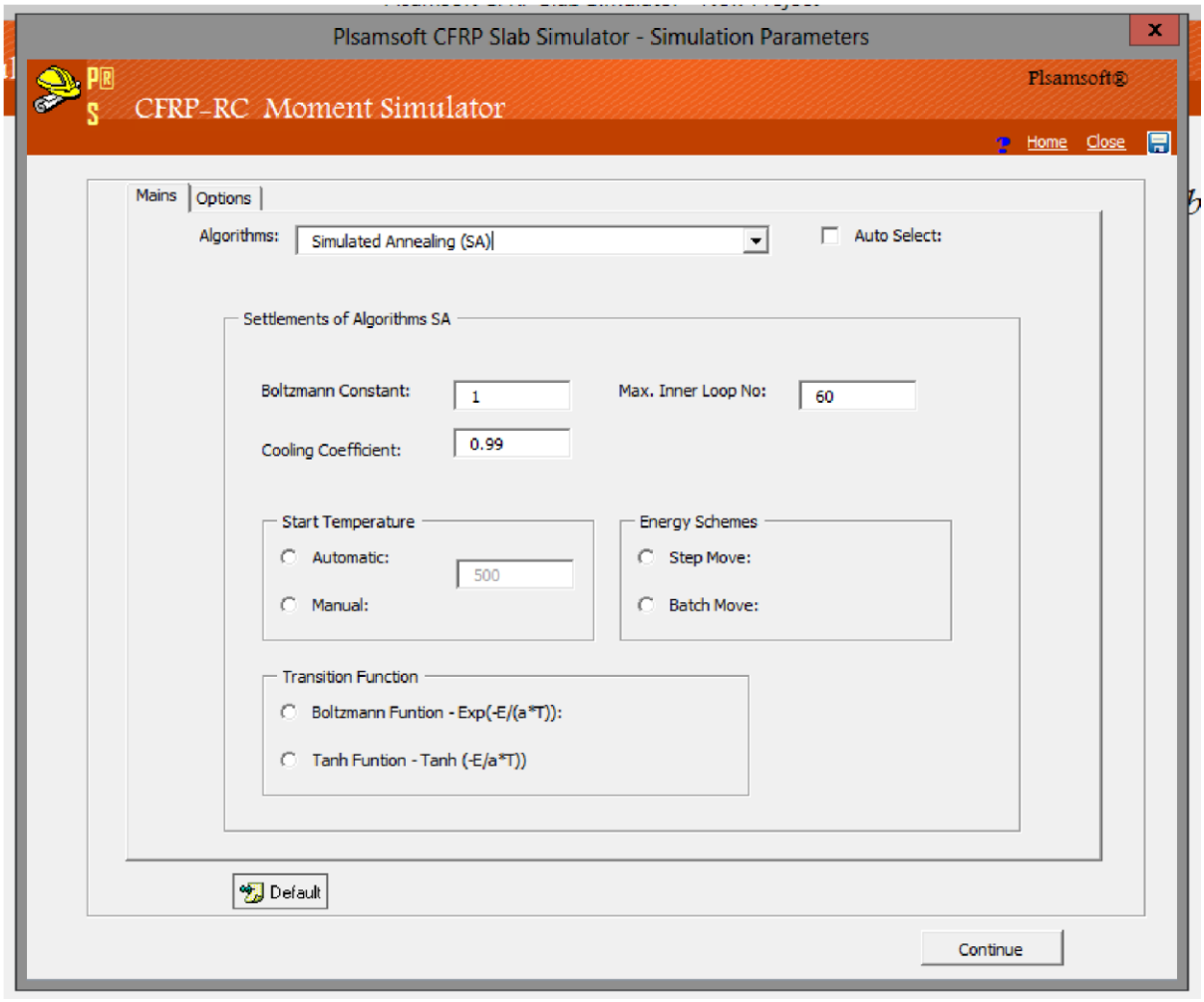


Figure 4.2: *Interface for Simulated Annealing Input Parameters*

The second interface that comes up when using the developed application is shown in Figure 4.2, this interface is used for inputting parameters which define the annealing starting temperature (T_0), number of iterations (niter), temperature reducing rate (c) and number of variables (nvar), these parameters guide the annealing part. Each of the input boxes is linked to the VBA code and

sends the values inputted by the user to the codes for execution. The command button "Continue" activates the next user
interface.
The lower and upper bound values of the above variables used are given in Table 4.1.

TABLE 4.1: LIMI TING VALUES OF ASSUMED VARIABLES

S/N	Limiting Values	Width of Slab *b (mm)*	Effective depth of Slab *d(mm)*	Diameter of CFRP $d_f(mm)$	Compressive Strength of Concrete $f_c'(kN/mm^2)$
1	Lower Bound Values	1000	50	4	20
2	Upper Bound Values	1000	250	22	50

Width of slab is defined in the program as unity and it is taken as 1000 mm, effective depth of slab is taken in a range between 50 to 200 mm as most practical slabs are designed in this range. Diameter of CFRP is taken to range between 4 to 22 mm because this is the range of currently available CFRP bars. Concrete compressive strength is taken between 20 to 50kN/mm^2. The program searches within this defined ranges for an optimum value of the resistance moment and returns the values as the results in Table 4.2
The parametric study results of the algorithm are shown in Table 4.2 and Figure 4.3.
It is seen that the final values of objective function (the moment capacity given by $k_{opt} = maximise\ \left[\frac{M_u}{bd^2 f_{cu}}\right]$), improves from the initial stage (0.125694) to the final

one (0.194578) with increase in the number of iterations.
For each iteration number, the program randomly selects values for the effective depth, concrete strength and CFRP diameter, and then it proceeds to calculate the reinforcement ratio and CFRP area. After some comparison on which should govern the failure type, it calculates the moment capacity and outputs it in the moment capacity column. The program runs until it finds a steady maximum value for the resistance moment capacity and reaches the maximum number of iterations before stopping.

TABLE 4.2: OPTIMAL MOMENT CAPACITY RESULTS USING SIMULATED ANNEALING

Iteration No.	**Effective Depth *(mm)***	**Slab Width *(mm)***	**Concrete Strength**	**CFRP Diameter *(mm)***	**Reinf. Ratio**	**CFRP Area (mm^2)**	**Ultimate Moment $\times 10^6 KNm$**	**Moment Capacity**	**Failure Type**
100	142.0	1000	26	18	0.0017	254.502	65.897	0.125694	Conc. Crushing
200	150.5	1000	25	17	0.0015	227.009	70.485	0.124475	CFRP Rupture

300	135.0	1000	24	22	0.0028	380.182	68.494	0.156594	Conc. Crushing
400	137.0	1000	24	22	0.0027	380.182	70.141	0.155711	Conc. Crushing
500	105.0	1000	20	22	0.0036	380.182	41.251	0.187079	Conc. Crushing
600	109.5	1000	20	21	0.0031	346.406	42.718	0.178135	Conc. Crushing
700	105.0	1000	20	22	0.0036	380.182	41.251	0.187079	Conc. Crushing
800	94.0	1000	20	22	0.0040	380.182	34.386	0.194578	Conc. Crushing
900	96.0	1000	20	22	0.0040	380.182	35.600	0.194578	Conc. Crushing
1000	94.0	1000	20	22	0.0040	380.182	34.386	0.194578	Conc. Crushing

It can be seen from Table 4.2, that the effective depth of the slab and the CFRP diameter have a greater influence on the moment capacity than the concrete strength. At a CFRP diameter of 17mm, the section failed by CFRP rupture but at a higher diameter, failure was by concrete crushing.

Figure 4.3 shows the result of the simulation as printed out by the program, it also shows the total iteration number, the algorithm used in the simulation, the start temperature and also the reason why the simulation was terminated which in this case was because the optimal value of the objective function was achieved.

Iteration No.	Effective Depth mm	Slab Width mm	Concrete Strength N/mm^2	CFRP Diameter mm	Reinf. Ratio	CFRP Area mm^2	Ultimate Moment Nmm	Moment Capacity	Failure Type
100	142	1000	26	18	0.001792268	254.502	65896962.9	0.125694236	Conc. Crushing
200	150.5	1000	25	17	0.001508369	227.0095	70484446.42	0.12447447	CFRP Rupture
300	135	1000	24	22	0.002616163	380.182	68934144.82	0.155592683	Conc. Crushing
400	137	1000	24	22	0.002775051	380.182	70141137.33	0.155711406	Conc. Crushing
500	105	1000	20	22	0.003620781	380.182	41250829.48	0.187078592	Conc. Crushing
600	109.5	1000	20	21	0.003163521	346.4055	42717644.98	0.178134922	Conc. Crushing
700	105	1000	20	22	0.003620781	380.182	41250829.48	0.187078592	Conc. Crushing
800	94	1000	20	22	0.00404489	380.182	34385886.3	0.194578352	Conc. Crushing
900	96	1000	20	22	0.00404489	380.182	35599653.1	0.194578352	Conc. Crushing
1000	94	1000	20	22	0.00404489	380.182	34385886.3	0.194578352	Conc. Crushing

Optimal Moment Capacity Results Using Simulated Annealing

Figure 4.3

Figure 4.4 shows the plot of the performance of the algorithm. At the initial stage, the variation of the objective function is too high. As the temperature parameter reduces, the variation is also

reduced and convergence is achieved at the culminating stage, hence the objective function converges to a steady and maximum value.

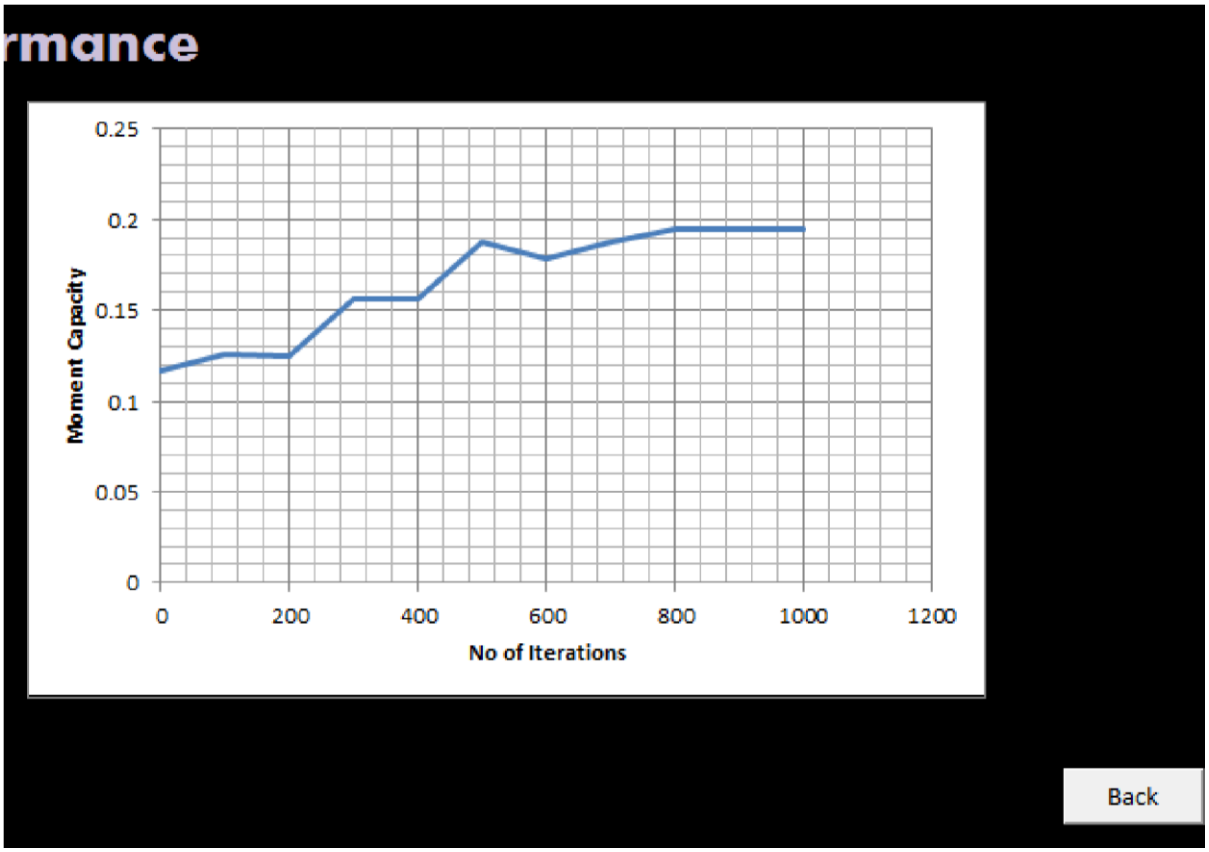


Figure 4.4 *: Performance of the simulated annealing Program*

The objective function for optimization is the maximization of ultimate moment capacity of a singly reinforced CFRP concrete slab subjected to bending. Equations have been formulated as given earlier in (Equations 3.1 to 3.10). The program is designed to read the required data, that is, limiting values of variables, and simulated annealing parameters as it applies the necessary constraints. The program then searches for a maximum for the objective function in the space of the four variables' limiting values.

The maximum of the objective function is recorded if all the constraints are satisfied. If any of the constraint is violated, the penalty for violation is given and the objective function modified by the penalty factor as defined by the user. The modified objective function incorporating the constraint violation is given in Equation (3.16).

The simulation resulted in an optimal value of **0.194** for the moment capacity of the assumed CFRP singly reinforced concrete slab section. This value when replaced for k_{opt} in the objective function, $k_{opt} = \text{maximise}\left[\frac{M_u}{bd^2 f_{cu}}\right]$ gives the optimum resistance moment (M_{opt}) of CFRP singly reinforced concrete sections as

$M_u = 0.194bd^2f_{cu}$.

CHAPTER FIVE

SUMMARY, CONCLUSIONS AND RECOMMENDATIONS

5.1 Summary

The use of CFRP in civil engineering applications enables engineers to obtain significant achievements in the functionality, safety and economy of construction concrete structures. The variabilities inherent in the CFRP materials, fabrication, and analysis method are investigated to carry out the optimization of the resistance moment of CFRP reinforced concrete sections. The ACI 440.1R-06, (2006), is used with a wide range of variables (slab breadth and depth, concrete strengths, cross-sectional dimensions and CFRP bar diameter) to develop resistance models for CFRP singly reinforced concrete slabs. An algorithm based on simulated annealing was used to optimize the developed models and the algorithm implemented using Visual Basic for Applications.

In summary, this study resulted in an optimal value of **0.194** as the moment capacity of CFRP singly reinforced concrete slabs. These results can be used to enhance the current recommendations for moment resistance of CFRP singly reinforced concrete slabs.

5.2 Conclusions

The primary aim of this work is to simulate the resistance moment of CFRP reinforced concrete slabs using annealing models in order to extend the existing knowledge of slabs with fiber reinforced polymers bars as the reinforcement. From the analytical studies and the formulations for the Simulated Annealing-based optimal moment resistance of CFRP concrete slabs along with identification of the objective function, constraints and design variables, the following conclusions are obtained.

1. This study resulted in an optimal value of **0.194** as the moment capacity of CFRP slabs.

2. With the results from this study, the optimal resistance moment of CFRP reinforced concrete slabs can be well understood since every single step of the optimization process was reported accurately in a well formatted manner and respective graphs also plotted to accuracy.

3. Higher moment of resistance was observed in compression failures (concrete crushing) as compared to a tension failure (CFRP rupture) as seen in Table 4.2.

4. The current ACI 440.1R-06 (2006) equations for nominal moment of reinforced concrete sections reinforced with CFRP can be modified with the findings in this work.

5. The ultimate moment resistance of slabs increases with the amount of CFRP rebars. This is true, obviously, for the case in which the failure mode is compression controlled (crushing of the concrete); this confirms the results of Ezeldin, (1992).

6. The developed simulated annealing successfully led the randomly distributed initial design points in the design space to the local optimum design point, hence providing an excellent convergence of the maximization process.

7. The optimum design results can well be controlled by the designer by specifying various design requirements.
8. The efficiency of the algorithm suggests its immediate application to other design optimization problems.

5.3 Recommendation and Suggestions

5.3.1 Recommendation

It is recommended in this work that the resistance moment of CFRP singly reinforced concrete slabs can be safely expressed as

$$M_u = 0.194bd^2f_{cu}$$

5.3.2 Suggestions for Future Research Work

The following suggestions are made for future research

1. This study focuses exclusively on the flexural behavior of CFRP singly reinforced concrete slab sections and assumes that the other modes of failure such as shear failure and bond failure do not control the analysis and design. Similar kind of research can be conducted for other modes of failure.

2. Further research should be pursued prior to allowing the use of CFRP as reinforcement for reinforced concrete slabs.

3. The developed computer program is based on the simulated annealing algorithm and it was implemented using visual basic; it would be interesting to consider other types of optimization techniques like Genetic Algorithm (GA), Ant Hill Colony (AHC) and Particle Swarm Optimization (PSO) and other programing languages like C++ and java to develop the program. This will go a long way to improve the result of the optimized resistance moment.

4. Designers as well as researchers should begin to consider unconventional failure modes (other than conventional flexural tension failures) in light of the fact that both flexural tension and flexural compression failure involve two brittle materials, i.e., concrete and CFRP.

REFERENCES

ACI Committee (2006). Guide for the Design and Construction of Concrete Reinforced with FRP Bars. ACI 440.1R-06. Farmington Hills: *American Concrete Institute,* Farmington Hills Michigan, USA, pp.243-250.

ACI Committee 440 (2001). Guide for the Design and Construction of Concrete Reinforced with FRP Bars, ACI 440.1R-01. *American Concrete Institute*, Farmington Hills, Michigan, USA:41.

ACI Committee 318 (2002), Building Code Requirements for Reinforced Concrete and Commentary, ACI 318-02, *American Concrete Institute*, Detroit, pp.63-65.

Adamu, A and Karihaloo, B. L, (1994), Minimum Cost Design of Reinforced Concrete Beams Using Continuum-type Optimality Criteria, *Structural Optimization*:91-102.

Achillides, Z. (1997), Bond Behavior of FRP Bars to Concrete, Proceedings of the Third International Symposium (FRPRCS-3), Sapporo*, Japan Concrete Institute*, 2:341-348.

Amy, K., (2002), Design Methods for FRP-Strengthened Concrete Using Sheets or Near- Surface Mounted Bars, *University of Manitoba*: 67-76

Bajpai, K., and Duthinh, D. (2003), Bending Performance of Masonry Walls Strengthened with Near-Surface Mounted FRP Bars, *9th North American Masonry Conference*, Clemson, USA.

Benmokrane, B., Ahmed, E. A., and El-Salakawy, E. F., (2010), Performance Evaluation of GFRP Shear Reinforcement in Concrete Beams, *ACI Structural Journal*, 107(1): 53-62.

BS 8110 (1985). The Structural Use of Concrete Part 1: 1985 and Part 2: 1985. Her Majesty's Stationary and File, London.

Chajes, M., Januszka, T., Mertz, D., Thomson, T., and Finch, W., (1995), Shear Strengthening of Reinforced Concrete Beams Using Externally Applied Composite Fabrics, *ACI Structural Journal*, 92(3): 60-63.

Chen, P. W., and Chung, D. A., (1996), Comparative Study of Concretes Reinforced With Carbon, Polyethylene, and Steel Fibers and Their Improvement by Latex Addition. *ACI Materials Journal*, March-April, 93(2): 129-133.

Clarke, J. L., and O' Regan, D. P. (1995) "Design of Concrete Structures Reinforced with Fiber Composite Rods" Proc., Non-Metallic (FRP) Reinforcement for Concrete Structures (FRPRCS-2), E & FN Spon, London, Great Britain, pp.646-653

Clarke J. L., O'Regan D. P. and Thirugnanenedran C., (1996), "EUROCRETE Project, Modification of Design Rules to Incorporate Non-ferrous Reinforcement", EUROCRETE Project, Sir William Halcrow & Partners, London, pp.64.

Coello, C.A., Christiansen, A. D. and Santos, F., (1997), A Simple Genetic Algorithm for the Design of Reinforced Concrete Beams, *Engineering with Computers,* 13, pp. 185-196.

Cohn, M. Z. and Lounis, Z., (1994), Optimal Design of Structural Concrete Bridge Systems, *ASCE Journal of Structural Engineering,* 9(120): 2653-2674.

Cohn M. Z. and Dinovitzer A. S., (1994) Application of Structural Optimization, *ASCE Journal of Structural Engineering*, 120(2): 617-649.

Cosenza, E., Manfredi, G., Realfonzo, R., (1997), Behavior and Modeling of Bond of FRP Rebars to Concrete, *Journal of Composites for Construction*, 1(2): 19-21.

Cooper, G. A., Aveston, J., and Kelly, A., (1971), Single and Multiple Fracture in The Properties of Fiber Composites, *Conference Proceedings*, National Physical Laboratory, Guildford. IPC Science and Technology Press Ltd, Surrey, England, pp.15-26.

CSA-S806-02, (2002), Design and Construction of Building Components with Fiber Reinforced Polymers. Rexdale: *Canadian Standard Association*.

El-Salakawy, E. and Benmokrane, B., (2004), Serviceability of Concrete Bridge Deck Slabs Reinforced with Fiber-Reinforced Polymer Composite Bars, *ACI Structural Journal*, 101(5):727-736.

El-Mihilmy, M, Manfredi, G, and Cosenza, E, (2000), Experimental Response and Code Models of GFRP RC Beams in Bending, *Journal of Composites for Construction*, November, 4(4): 182-190.

El-Mihilmy, M., and Tedesco J., (2000), Analysis of Reinforced Concrete Beams Strengthened with FRP Laminates, *Journal of Structural Engineering*, 126(6): 76-85.

Esfahani, R., Kianoush, R., and Lachemi, M., (2005), Bond Strength of Glass Fiber Reinforced Polymer Reinforcing Bars in Normal and Self-Consolidating Concrete, *Canadian Journal of Civil Engineering*, 32(3): 38-45.

Ezeldin, A, Cheng- T. and Thomas Hsu. (1992), Optimization of Reinforced Fibrous Concrete Beams, *ACI Journal of Structural Engineering,* 1(89): 106-14.

Ferreira A., Camanho P., Marques A., and Fernandes A., (2001), Modeling of Concrete Beams Reinforced with FRP Rebars, Composite Structures, 53.

Grace, N. and Singh, S., (2003), Design Approach for Carbon Fiber-Reinforced Polymer Prestressed Concrete Bridge Beams, *ACI Structural Journal*, 100(3): 80-88

Hwan, B., (1992), Flexural Analysis of Reinforced Concrete Beams Containing Steel Fibers, *Journal of Structural Engineering, ASCE,* 10(118): 2821-2835.

Ingber, L. (1995), Adaptive Simulative Annealing (ASA), Lessons Learned. Invited Paper to a special issue of the Polish Journal Control and Cybernetics on Simulated Annealing Applied to Combinatorial Optimization.

Jenkins, W. M., (1992), Plane Frame Optimum Design Environment Based on Genetic Algorithm, *ASCE Journal of Structural Engineering*, 118(11): 3103-3112.

Kirkpatrick, S., Gelatt, C. D. Jr. and Vecchi, M. P. (1983), Optimization by Simulated Annealing, *Science*,4598(220):671-80.

Kocaoz S., Samaranayake V., and Nanni A., (2005), Tensile Characterization of Glass FRP Bars, Composites, Part B, 36.

Li, V., and Wang, S., (2002), Flexural Behaviors of Glass Fiber-Reinforced Polymer

(GFRP) Reinforced Engineered Cementitious Composite Beams, *ACI Materials Journal*, 99(1): 38-78.

Löfgren, I. (2005), Fibre reinforced Concrete for Industrial Construction – A Fracture Mechanics Approach to Material Testing and Structural Analysis. Unpublished PhD Thesis, Chalmers University of Technology, Göteborg.

Lorenzis, L. and Nanni, A., (2002), Bond between Near Surface Mounted FRP Rods and Concrete in Structural Strengthening, *ACI Structural Journal*, 99(2): 90-97.

Malvar, J. L., (1994), Technical Report: Bond Stress Slip Characteristics of FRP Bars, Naval Facilities Engineering Service Center, Port Hueneme, CA, Feb, p. 45;

Michael, J. G., (1997), Chapter 3: Materials, Reinforced Concrete: Mechanics and Design, Third Edition, Prentice Hall, New Jersey, pp. 35-81.

Nanni, A. (1999), Composites: Coming on Strong, *Concrete Construction*, 44(1): 120-124

Narayanan, R. and Darwish, I. Y. S. (1987), Use of Steel Fibers as Shear Reinforcement. *ACI Structural Journal*, 84(3): 216_227.

Nawy, N., Edward G., and Gary, E. (1977), Fibre Glass Reinforced Concrete Slabs and Beams, *Journal of Structural Division*, (103): 421-439.

Newhook, J., Ghali, A., and Tadros, G., (2002), Concrete Flexural Members Reinforced with Fiber Reinforced Polymer: Design for Cracking and Deformability," *Canadian Journal of Civil Engineering*, 29: 125-134.

Pecce, M., Manfredi, G., and Cosenza, E., (2000), Experimental Response and Code Models of GFRP RC Beams in Bending, *Journal of Composites for Construction,* 4(4): 425-438.

Plevris, N., Triantafillou, T. C., and Veneziano, D., (1995), Reliability of RC members strengthened with CFRP laminates, *Journal of structural engineering, ASCE*

Rajeev, S. and Krisnamoorthy, C. S. (1992), Discrete optimization of structures using genetic algorithms, *ASCE Journal of Structural Engineering*, 118(5): 1233-1250.

Rostasy, F. S. (1996), Bonding of Steel and GFRP Plates in the Area of Coupling Joints. Talbrucke Kattenbusch. Research Report No. 3126/1429, *Federal Institute for Materials Testing*, Braunschweig, Germany.

Rostasy, F.S. (1997), "On Durability of FRP in Aggressive Environments," Proceeding of the Third International Symposium on Non-Metallic (FRP) Reinforcement for Concrete Structures (FRPRCS-3), *Japan Concrete Institute*, Tokyo, Japan, 2: 107-114.

Sarma, K. C. and Adeli, H., (1998), Cost optimization of concrete structures, *ASCE Journal of Structural Engineering*, 124(5): 570-578.

Seible, F. and Karbhari, V.M., (1996), Fiber Reinforced Composites, *Advanced Materials for Renewal of Civil Infrastructure*. Appl. Comp. Mater. **7**, pp.95-124.

Sivagamasundari, R., and Kumaran, G. (2008) "A Critical Study on the Suitability of Glass Fiber Reinforced Polymer Reinforcements for Concrete One Way Slabs," in International Conference on Recent Developments in Structural Engineering, *Manipal Institute of Technology*, Manipal , India, pp.265.

Soroushian P. and Bayasi Z. (1991). Fiber-type Effects on the Performance of Steel Bar Reinforced Concrete, *ACI Materials Journal*, 88(2): 129-34.

Tang, B., (1999), Fiber Reinforced Polymer Composites Applications in USA," *First Korea/U.S.A*. *Road Workshop Proceedings*, January: 28-29.

Thiagarajan, G., (2003), Experimental and Analytical Behavior of Carbon FiberBased Rods as Flexural Reinforcement, *Journal of Composites for Construction*, 7(1): 56-66.

Toutanji, H. A. and Saafi, M., (2000), Flexural Behavior of Concrete Beams Reinforced with Glass Fiber-Reinforced Polymer (GFRP) Bars", *ACI Structural Journal,* 12(7): 58-60.

Triantafillou, T., and Antonopoulos, C., (2000), Design of Concrete Flexural Members Strengthened in Shear with FRP, *Journal of Composites for Construction*, 4(4): 70-77.

Whitehead, P. and Ibell, T. J., (2001). Shear Behavior of FRP-prestressed Concrete

Beams. In: 5th International Conference on The Use of FRPs in Reinforced Concrete Structures, Cambridge.

Yepes, V. and Medina, J. R., (2006), Economic Heuristic Optimization for the Heterogeneous Fleet VRPHESTW. *ASCE Journal of Transportation Engineering*, 132(4): 303-311.

Yost, J. R. (1993) "Fiber Reinforced Plastic Grids for the Structural Reinforcement of Concrete Beams" PhD Dissertation, University of New Hampshire, Durham, N.H.

APPENDIX

Compressed Simulated Annealing VBA Code.

```
Private Sub cmdExit_Click()
End
End Sub
```

```
Private Sub Optimisation_Click() Close
‘Enter data from UserForm
Dim IT As Double, LMC, DR, DT, ML, AR, NR
IT = txtIT.Text
LMC = txtLMC.Text
DR = txtDR.Text
DT = txtDT.Text
ML = txtML.Text
AR = txtAR.Text
NR = txtNR.Text
Dim R as Double, POWER, Pacc, Temp
'Maximum number of annealing runs is 50
If NR > 50 Then
NR = 50
End If
R = 1
While R < NR + 1
Sheets("SA").Cells(6, 4) = R
Dim NPVb(500) As Integer 'define matrix that measures if solution has converged
Temp = IT ‘define initial temperature
Sheets("SA").Cells(4, 2) = Temp ‘print temperature to worksheet
Sheets("SA").Activate ‘activate the sheet
Dim SAM(480) As Integer ‘construct string representing matrix
For J = 1 To 480 ‘fill SAM matrix with random binary numbers
Randomize ‘this command initialises the random number generator by giving it a new seed
value
SAM(J) = Int(2 * Rnd)
Next
'Print matrix to worksheet
For J = 1 To 480
ColM = 1 + (J Mod 20) ‘this command allows the string to be printed as a matrix to the
worksheet If ColM = 1 Then
ColM = 21 'this loop corrects an error associated with use of Mod function End
If
Sheets("SA").Cells(8 + ((J - 1) \ 20), ColM) = SAM(J)
Next
Dim NPVo As Single, NPVn, TError, NA, NT, L
L=0 ‘initial lambda for penalty function is zero
Sheets("SA").Cells(4, 4) = L ‘print lambda to sheet
I = 0 ‘iteration number
Sheets("SA").Cells(2, 4) = I ‘print iteration number to sheet
NPVo = Sheets("SA").Cells(3, 2) 'get NPV value from worksheet
TError = Sheets("SA").Cells(3, 4) 'get number of errors from worksheet AFo =
NPVo - TError * L 'calculate augmented functional
```

```
Do Until Temp < 0.0001 ‘run outer loop until temperature is less than epsilon
NA = 0 ‘initialise number of acceptances
NT = 0 ‘initialise number of trials
Do
Sheets("SA").Cells(5, 2) = NT ‘print to worksheet
Randomize 'these lines of code randomly select a cell for updating
CurCell = Int((480 * Rnd) + 1)
‘Swap its binary value
If SAM(CurCell) = 0 Then
SAM(CurCell) = 1
Else
SAM(CurCell) = 0
End If
ColM = 1 + (CurCell Mod 20) 'print updated cell to worksheet
If ColM = 1 Then
ColM = 21 'This loop corrects an error associated with use of Mod function End
If
Sheets("SA").Cells(8 + ((CurCell - 1) \ 20), ColM) = SAM(CurCell)
NPVn = Sheets("SA").Cells(3, 2) 'get profit associated with new configuration from worksheet
TError = Sheets("SA").Cells(3, 4) 'also get number of errors associated with new solution
from worksheet
AFn = NPVn - TError * L ‘calculate new augmented functional
If AFn >= AFo Then 'always accept higher augmented profit
AFo = AFn
Sheets("SA").Cells(2, 2) = AFo
NA = NA + 1 ‘number of acceptances is increased by one
Sheets("SA").Cells(6, 2) = NA ‘print number of acceptances to worksheet Else
POWER = (AFn - AFo) / Temp ‘if augmented profit is not higher, construct Boltzmann acceptance
criterion
Pacc = Exp(POWER)
End If
Randomize
If Pacc > Rnd Then ‘test solutions using stochastic acceptance function of annealing theory
AFo = AFn 'Update iterates
Sheets("SA").Cells(2, 2) = AFo
NA = NA + 1
Sheets("SA").Cells(6, 2) = NA
Else 'undo change
If SAM(CurCell) = 1 Then
SAM(CurCell) = 0
Else
SAM(CurCell) = 1
End If
‘Print updated cell to worksheet
```

```
ColM = 1 + (CurCell Mod 20)
If ColM = 1 Then
ColM = 21 'This loop corrects an error associated with use of Mod function End
If
Sheets("SA").Cells(8 + ((CurCell - 1) \ 20), ColM) = SAM(CurCell)
End If
End If
If NA = Int(LMC * AR) Then Exit Do ‘break inner loop if number of acceptances reaches
upper bound
If NT = 480 Then Exit Do ‘break inner loop if number of trials reaches upper bound
NT = NT + 1 ‘otherwise increase number of trials by one and begin inner loop again A =
Timer
While Timer < A + 0.005
DoEvents
Wend
Loop
NPVb(I) = AFo ‘enter profit term into convergence matrix
If I > 10 Then 'break loop if augmented profit has converged
If NPVb(I - 8) = NPVb(I - 9) Then
If NPVb(I - 7) = NPVb(I - 8) Then
If NPVb(I - 6) = NPVb(I - 7) Then
If NPVb(I - 5) = NPVb(I - 6) Then
If NPVb(I - 4) = NPVb(I - 5) Then
If NPVb(I - 3) = NPVb(I - 4) Then
If NPVb(I - 2) = NPVb(I - 3) Then
If NPVb(I - 1) = NPVb(I - 2) Then
If NPVb(I) = NPVb(I - 1) Then Exit Do
End If
End If
End If
End If
End If
End If
End If
End If
End If
End If
I = I + 1 ‘increase iteration count by one
L = ML * (1 - Exp(-DL * I)) ‘update penalty factor
Temp = Temp * DT
Sheets("SA").Cells(2, 4) = I ‘print updated values to worksheet
Sheets("SA").Cells(4, 2) = Temp
Sheets("SA").Cells(6, 2) = 0
Sheets("SA").Cells(4, 4) = L
Loop
```

```
Sheets("NPV").Activate
Sheets("NPV").Cells(R + 1, 2) = AFo
Sheets("NPV").Cells(R + 1, 3) = TError
Sheets("NPV").Cells(R + 1, 4) = L
Sheets("NPV").Cells(R + 1, 5) = I
Sheets("Output").Activate
'Print matrix to worksheet
For J = 1 To 480
ColM = 1 + (J Mod 20)
If ColM = 1 Then
ColM = 21 'This loop corrects an error associated with use of Mod function End
If
Sheets("Output").Cells((25 * (R - 1) + 2) + ((J - 1) \ 20), ColM) = SAM(J) Next
R = R + 1 ‘this updates the run counter, the algorithm subsequently starts at the next run at
top of sheet Wend
Close
End Sub
Private Sub UserForm_Activate()
txtIT.Text = 903
txtLMC.Text = 480
txtDR.Text = 0.04
txtDT.Text = 0.925
txtML.Text = 413
txtAR.Text = 0.5 txtNR.Text
= 1
End Sub
```